skb.se

SKB R-25-18

ISSN 1402-3091
ID 2098714
October 2025

Effect of sulphide in water on the creep rate of Cu-OFP at room temperature

Kai Arstila, Ahsan Chonche, Tiina Ikäläinen, Timo Saario
VTT Technical Research Centre of Finland Ltd

Keywords: Cu-OFP, sulphide, creep rate

Summary

In this work, the main target was to investigate the source of the creep rate increase in Cu-OFP when exposed to sulphide containing water, occurring when the sulphide is removed from the water. From general grounds it was suggested that there are two possible sources for the phenomena, the first one being hydrogen egress/ingress and the second one injection of vacancies into the Cu-OFP, both capable of influencing dislocations to produce an increase in the creep rate.

The main conclusion from this work is that injection of vacancies into Cu-OFP is likely the cause of the observed increase in the creep rate when sulphide removal is started. The kinetics of the process is such that the rate of removal of sulphide from the water becomes an important parameter. Too high a rate of sulphide removal, such as having too high a bubbling rate of N_2 or replacing the sulphide containing water with fresh water without sulphide too rapidly, shows only a small or negligible increase in the creep rate. The N_2 bubbling by itself (i.e. through a mechanical action on the specimen) was shown not to produce a significant effect on the creep rate. The Cu-OFP material studied (tube 58) was found to have local variations in the hydrogen concentration, which prevented any firm conclusions to be made on the possible injection of hydrogen into Cu-OFP during the period of accelerated creep.

The oxygen enriched layer at the sulphide film – Cu-OFP interface observed by several research groups was shown to be caused by an artefact. The sulphide film is of a porous nature, allowing ingress of oxygen into the sulphide film – Cu-OFP interface during the post-exposure SEM sample preparation process.

As a separate finding from this work, the anodic current density of Cu-OFP at a potential 30 mV positive to the corrosion potential was found to correlate well with the sulphide concentration in the water (up to about 20 mg/l), thus providing a possible on-line sensor for sulphide concentration monitoring during experiments. It should be emphasized that this type of a sensor is not a universal one, since it is sensitive to the mass flow of sulphide onto the surface, which again is affected by the environmental conditions (e.g. static or flowing).

Content

1 Background

In previous work (Ikäläinen et al. 2022) it has been found that if Cu-OFP is exposed to sulphide (10^{-3} M, 32 mg/l) containing water during a creep test (constant load at 135 MPa), and the sulphide is then gradually removed from the water, the creep rate may undergo a dramatic increase by over 10 to 100 times. The creep rate increase was, however, found to be transient, lasting for a few tens of hours.

From general knowledge, two possible mechanisms have been suggested to explain the phenomena, i.e. ingress of vacancies into the Cu-OFP (possibly due to reductive dissolution of the sulphide film) or egress/ingress of hydrogen as a consequence of the sulphide removal from the water phase. Within the hydrogen egress hypothesis, reducing the sulphide concentration in the water would result in accelerated recombination of hydrogen atoms on the Cu-OFP surface, letting them escape into the gas volume as H_2 gas, and further letting the hydrogen in the near-surface layers of Cu-OFP to diffuse out thus helping to mobilize dislocations. Both vacancies and hydrogen are known to be able to increase the mobility of dislocations in metals, thus providing for the observed transient increase in the creep rate. It is likely that both mechanisms would affect preferentially the near-surface layers of Cu-OFP. The work described in this report aims at investigating the mechanism of the creep rate increase after starting the removal of sulphide from the water phase.

The targets for the different experiments in this work were as follows.

Experiments 1 and 2 were aimed to find out if the way of removing the sulphide from the water (i.e either N_2 bubbling or replacing the sulphide containing water with water without sulphide) has an effect on the creep rate behaviour.

Experiments 3 and 4 were aimed at revealing if the N_2 bubbling itself, through a mechanical action on the specimen (in the absence of sulphide) is able to cause the observed changes in the creep rate.

Experiment 5 was aimed at verifying the source of an oxygen enriched layer at the copper/sulphide film interface observed by several research groups in SEM cross-sections of Cu-OFP specimens previously exposed to sulphide containing water.

Experiment 6 was aimed to verify whether the oxide formation and reduction cycle produces an increase in the creep rate of Cu-OFP, in absence of sulphide.

Experiments 7 to 11 were aimed at revealing if hydrogen is injected into the Cu-OFP creep sample during N_2 bubbling after exposure to sulphide containing water, i.e. during the period of decreasing sulphide concentration in the water and elevated creep rate.

2 Experimental

The Cu-OFP material studied was delivered by SKB. The received material had approximate dimensions of 170x130x50 mm, cut from the tube T58. The material had been characterised and found to meet the post-production requirements. The average mechanical properties of nine samples representing different locations within the tube material are shown in Table 2-1. The average concentration of phosphorous and impurities is shown in Table 2-2.

Table 2-1 Average room temperature mechanical properties of the material (Välimäki 2009).

$Rp_{0.2}$ N/mm²	R_m N/mm²	Elongation %	Hardness HV5
42	212	52	43

Table 2-2 The average phosphorous and impurity concentration of the material, in wt-ppm (Välimäki 2009).

P ppm	S ppm	O ppm	H ppm
58.7	5.4	3.0	0.43

The Cu-OFP specimens had dimensions of 0.5 mm (thickness), 8 mm (width) and 29 mm (length of the deforming part of the body). The specimen design is shown in Figure 2-1. The specimens were manufactured using electric discharge machining (EDM). Before testing, the deforming part of the specimen body was polished (#220, #500 and #1200 SiC-papers successively) to remove the EDM affected surface layer. Thus, the actual specimen thickness was about 0.4 mm.

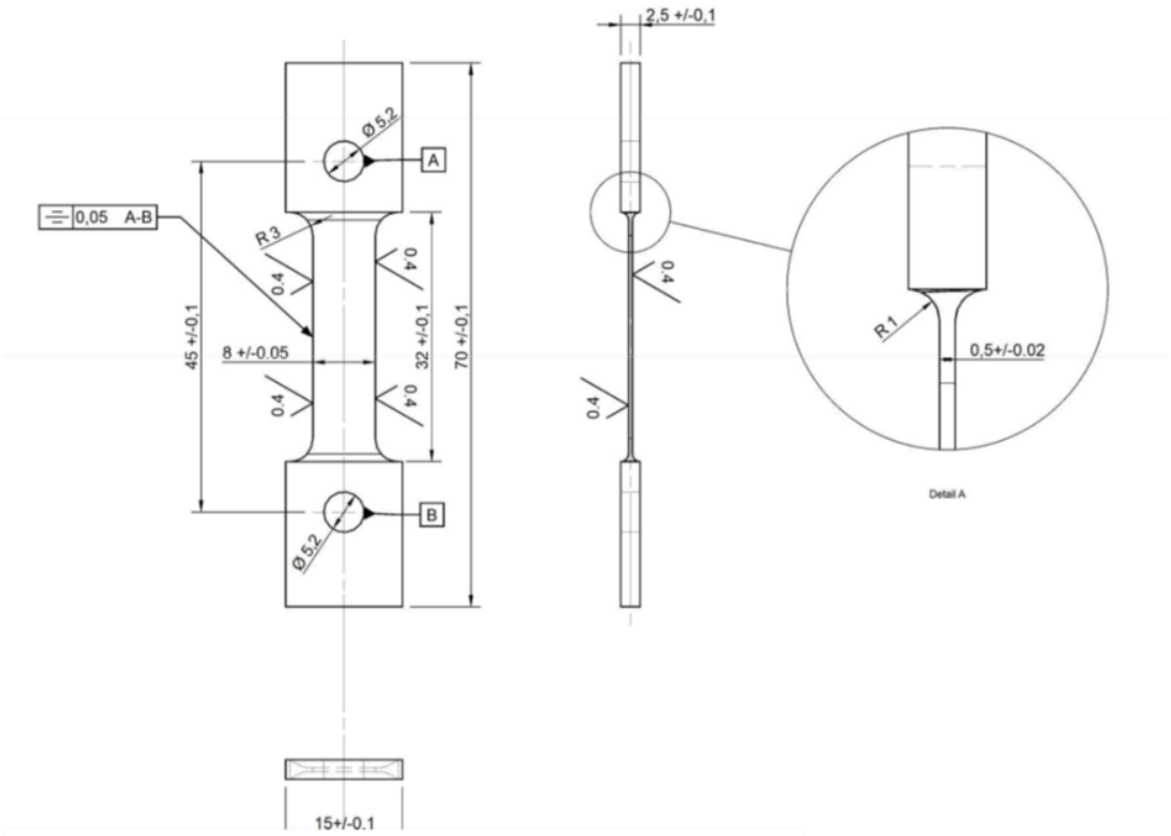

Figure 2-1. *Specimen design.*

The specimens were attached to the loading grips of a tensile machine, electrically insulated from the grips by ZrO_2 parts. The loading part was attached to an autoclave lid and placed inside the autoclave body. All autoclave parts were made of AISI 316L stainless steel. The pull rod extended through the autoclave lid via a Ballseal™ spring loaded sealing element, with a friction force of 59 N at room temperature. The autoclave was equipped with a Ag/AgCl(0.05 M KCl) reference electrode and a Pt counter electrode. An Autolab PGSTAT302F potentiostat with Nova 2.0 software was used to measure and control the potential and current of the specimen. The loading of the specimen was controlled by Cormet SSRT system v. 4.03.

Tests performed in sulphide containing water the experiments were performed in a stainless steel autoclave in a phosphate buffer ($Na_2HPO_4*2H_2O$ / $NaH_2PO_4*2H_2O$) solution of pH = 7.2. The sulphide addition (Na_2SxH_2O, 60-63%) was made at a target concentration of 32 mg/l (1 mM) to a

10 l glass stock vessel filled with the buffer solution, which was previously bubbled oxygen free with 5N N_2-gas (Aga Ltd). The glass stock vessel was pressurized to 0.5 bar overpressure with 5N N_2 to keep oxygen out and to balance the pressure drop caused by the outgoing water flow. After adding the sulphide, the autoclave was bubbled oxygen free with 5N N_2-gas and a tube pump (Cole-Parmer Instrument Co.) was used to pump the electrolyte through the autoclave. After flowing through the autoclave, the solution was directed to a 40 l storage tank where $FeCl_3*6H_2O$ was used to neutralize sulphide. The pH at the end of the experiment was measured at about pH = 7.3.

In a part of the tests, two 10 l stock vessels were used, the first one holding the buffer solution with the sulphide and the other one with buffer only. The two stock vessels were connected at the autoclave inlet with a three-way valve, allowing for a swift change from sulphide containing feed to buffer only. With this sequence, the pressure in the system will stay unchanged and thus the effect of a possible pressure increase due to introducing N_2 bubbling (and consequent load increase) in the creep rate can be excluded. The N_2 bubbling rate during the experiments was targeted at 1 bubble/second from a 6 mm diameter outlet tube, estimated to correspond to about 0.4 to 1 l/hr.

Loading of the specimen to the desired level was done only after the outlet sulphide level was confirmed to reach the sulphide target level.

The sulphide concentration was measured from the autoclave outlet from grab samples using Chemetrics C-9510D-kit for large concentrations (5 to 300 mg/L).

At the pH used in this experiment, about 45% of the sulphide is in the form of gaseous H_2S (Lilja 2021). Since no continuous bubbling through was used (only pressurization) gaseous H_2S was not able to escape from the stock solution and the sulphide concentration in the stock solution tended to stay constant.

Hydrogen concentration was measured with Hot Melt Extraction (HME)-technique using Bruker G8 ON/H MS device. In the tests involving hydrogen measurement of the samples, the specimen was removed from the autoclave, the sulphide film was removed by #220 SiC paper, the gauge length of the specimen was cut in two roughly equal pieces and immediately stored in a freezer (T = -18°C) to wait for the HME-measurement. The time from opening the autoclave into storing the specimen pieces into the freezer took less than 30 minutes.

With regard the scanning electron microscopy (SEM) studies, a field emission gun - scanning electron microscope (FEG-SEM) Zeiss Crossbeam 540 equipped with solid-state four-quadrant backscatter detector was used to characterize specimens.

The specimen cross sections were analysed by SEM-secondary electron (SE) imaging and backscatter electron (BSE) imaging. SE imaging was performed at a working distance (WD) of 10–15 mm with 15-20 keV, 1.5-3 nA. BSE images were acquired with the solid-state four-quadrant backscatter detector at 15-20 keV acceleration voltage with WD of 5–7 mm. Film layer chemical analysis was performed with SEM-Energy Dispersive X-Ray (EDX) with 20 keV, 3 nA. SE mode is more sensitive to surface layer topography. BSE imaging is based on the dependence of the backscatter electron signal on the orientation of crystal lattice planes with respect to incident electron beam due to electron channeling, thus is more sensitive on crystal structure and chemical composition.

3 Results

3.1 Experiment 1

The first test in sulphide involved first exposing the Cu-OFP under creep conditions to 32 mg/l (10^{-3} M) sulphide containing buffer (pH = 7.2) for about 48 hrs and then switching the feed into the same buffer without sulphide using a three-way connection in the feedwater line.

Two problems were encountered. The first one was not including the friction force of the sealing element in the load calculation, resulting in a lower stress level. This was corrected by increasing the load about 24 hrs into the experiment. The second one was that the gas flow line into the sulphide containing vessel was not closed when connecting the three-way connection to feed the buffer without the sulphide into the autoclave. This resulted in some of the sulphide containing buffer mixing into the pure buffer (about 2 mg/l).

Figure 3-1 shows the stress and elongation as a function of time, and

Figure 3-2Figure 3-2 the sulphide concentration and elongation as a function of time for the period of switching the source of buffer. The creep rate is seen to increase somewhat, to about double (from $2.8*10^{-8}$ s^{-1} to $6.5*10^{-8}$ s^{-1}), as a result of switching the buffer, but not nearly as much as previously (up to two orders of magnitude, when using N_2-bubbling to remove the sulphide). Also, the transient in creep only lasted for about two hours, instead of up to several tens of hours as previously found. Note that it took about 7.5 hours to reduce the sulphide level from 32 mg/l to the lowest level, i.e. 2 mg/l.

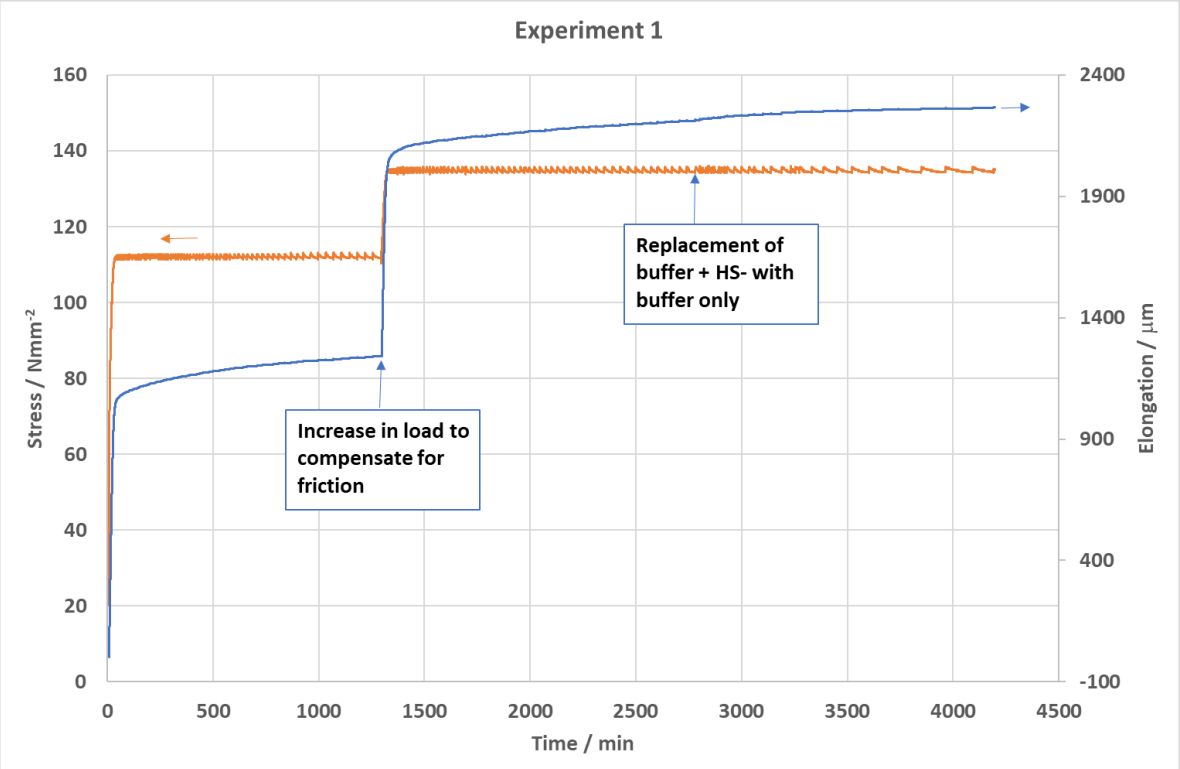

Figure 3-1. *Stress and elongation as a function of time.*

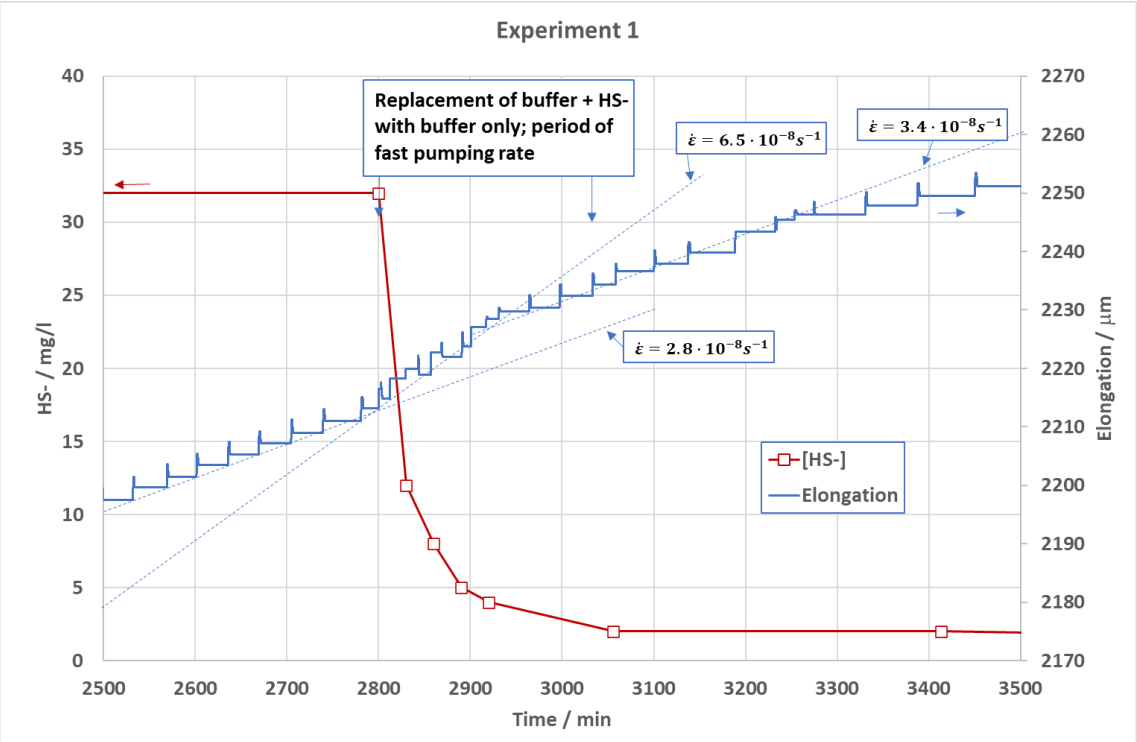

Figure 3-2. *Sulphide concentration and elongation as a function of time.*

Note that the rate of decrease in the HS- concentration seems much faster than the rate of increase in the elongation rate. This difference probably informs the rate at which defects are produced and diffusing versus the rate at which the environment is changing. This is supporting the mechanism of vacancy injection followed by slow diffusion. The hydrogen mechanism would be expected to produce more of a strain burst in defect production and movement.

During the test the corrosion potential was measured continuously up until the switch of the buffer source, showing a potential of about E = -0.65 VSHE. During the period of switching the buffer source it was decided to measure the polarization resistance periodically, with corrosion potential measured at the start of each polarization resistance measurement. The result is shown in Figure 3-3. A pronounced effect of decreasing sulphide concentration was observed in the anodic branch of the polarization resistance curve, so that the current density at the potential of 30 mV positive to the OCP decreased from about 0.06 mA/cm2 to about 0.01 mA/cm2 when going from about 30 mg/l to about 2 mg/l in sulphide. This is proposed to result from the anodic current density being controlled by the rate of diffusion of sulphide onto the sample surface. It would appear that measuring the anodic current density could provide a convenient on-line sensor for the sulphide concentration in the water phase. It should be emphasized that this type of a sensor is not a universal one, since it is sensitive to the mass flow of sulphide onto the surface, which again is affected by the environmental conditions (e.g. static or flowing).

Figure 3-4 shows the corrosion potential and sulphide concentration as a function of time (starting from switching the feed to buffer only). The corrosion potential was found to increase by about 60 mV during the period when sulphide concentration decreased from 30 to 2 mg/l.

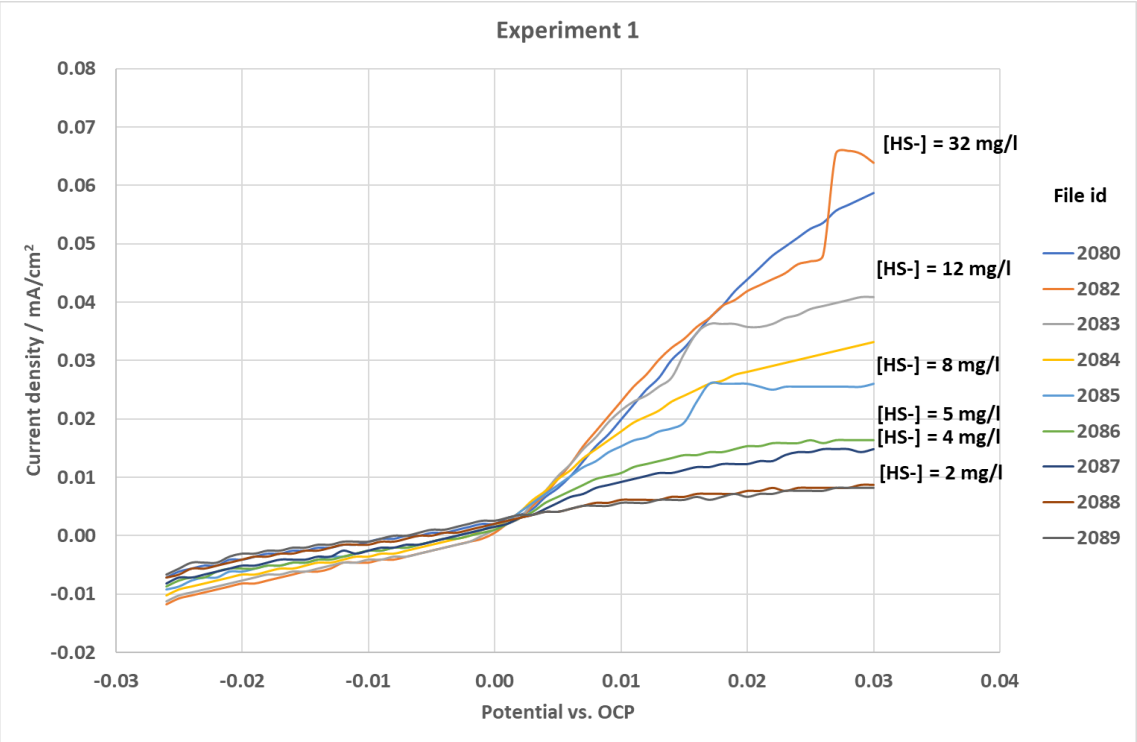

Figure 3-3. *Polarization resistance measurements during the period of switching the buffer source.*

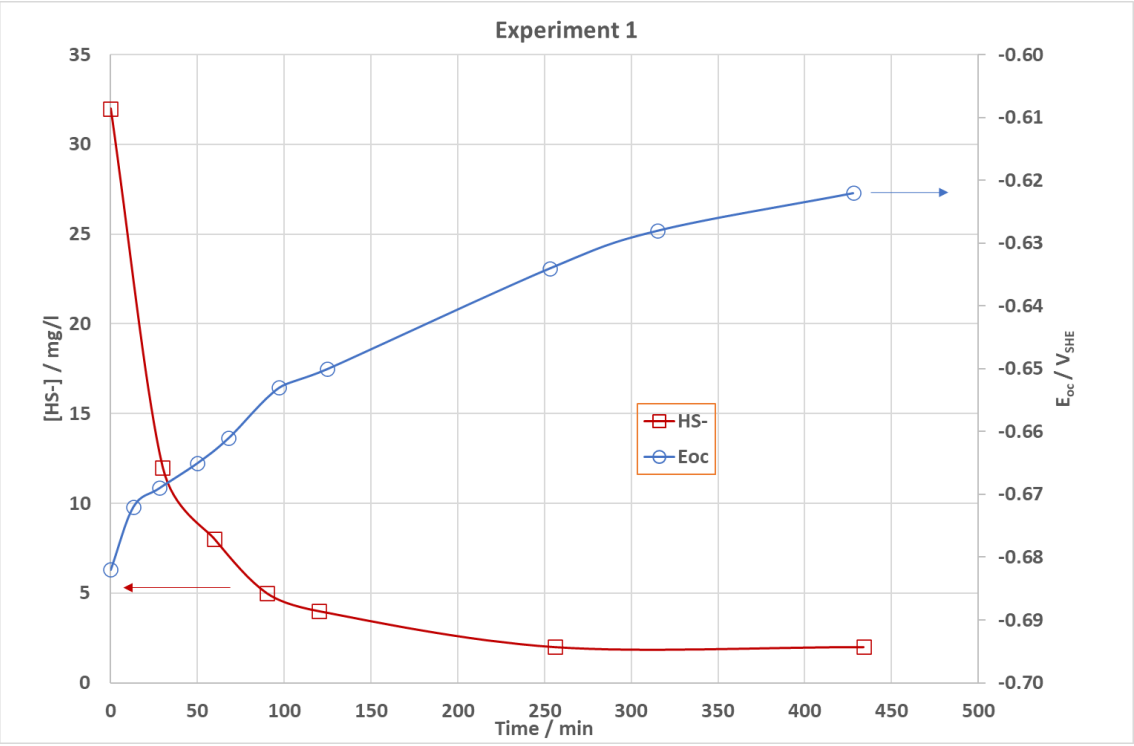

Figure 3-4. *Corrosion potential and sulphide concentration as a function of time (starting from switching the feed to buffer only).*

3.2 Experiment 2

This test in sulphide involved first exposing the Cu-OFP under creep conditions to 32 mg/l (10^{-3} M) sulphide containing buffer (pH = 7.2) for about 48 hrs and then switching the feed into the same buffer without sulphide using a three-way connection in the feedwater line.

An anomaly occurred in the creep behaviour of the sample so that there was some increase in the strain rate (blue curve) starting from about 900 min and slowly decreasing back to the previous level till about 2000 min, see Figure 3-5. There were no changes in the monitored parameters (sulphide concentration, corrosion potential or load) before or during this period. Thus it was concluded that the anomaly is related to some inhomogeneity in the Cu-OFP material.

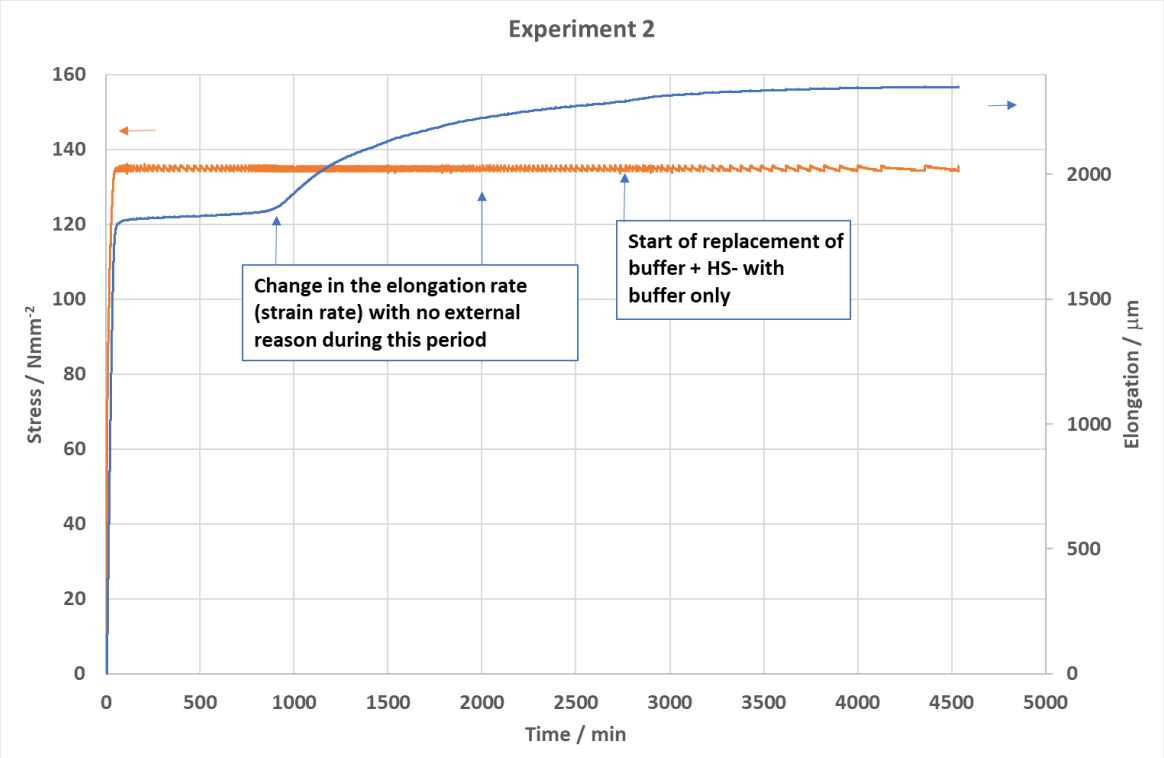

Figure 3-5. *Stress and elongation as a function of time.*

Figure 3-6 shows the sulphide concentration and elongation as a function of time for the period of replacing the buffer with sulphide with pure buffer solution. The creep rate is seen to increase somewhat, to about double (from $3.6*10^{-8}$ s^{-1} to $6.5*10^{-8}$ s^{-1}), as a result of switching the buffer, very closely the same as in Experiment 1. The strain rate is seen to decrease after sulphide has been removed to a slightly lower level than when sulphide was present. This is also similar to the result in Experiment 1. Note that, also similarly to Experiment 1, it took about 3.5 hours to reduce the sulphide level from 32 mg/l to about 2 mg/l.

In earlier experiments, the creep rate was seen to increase by a factor of up to x100 due to removal of sulphide by N_2-bubbling, while in these two experiments, when the sulphide was removed by replacing the buffer with sulphide with buffer only, the increase was limited to a factor of about x2.

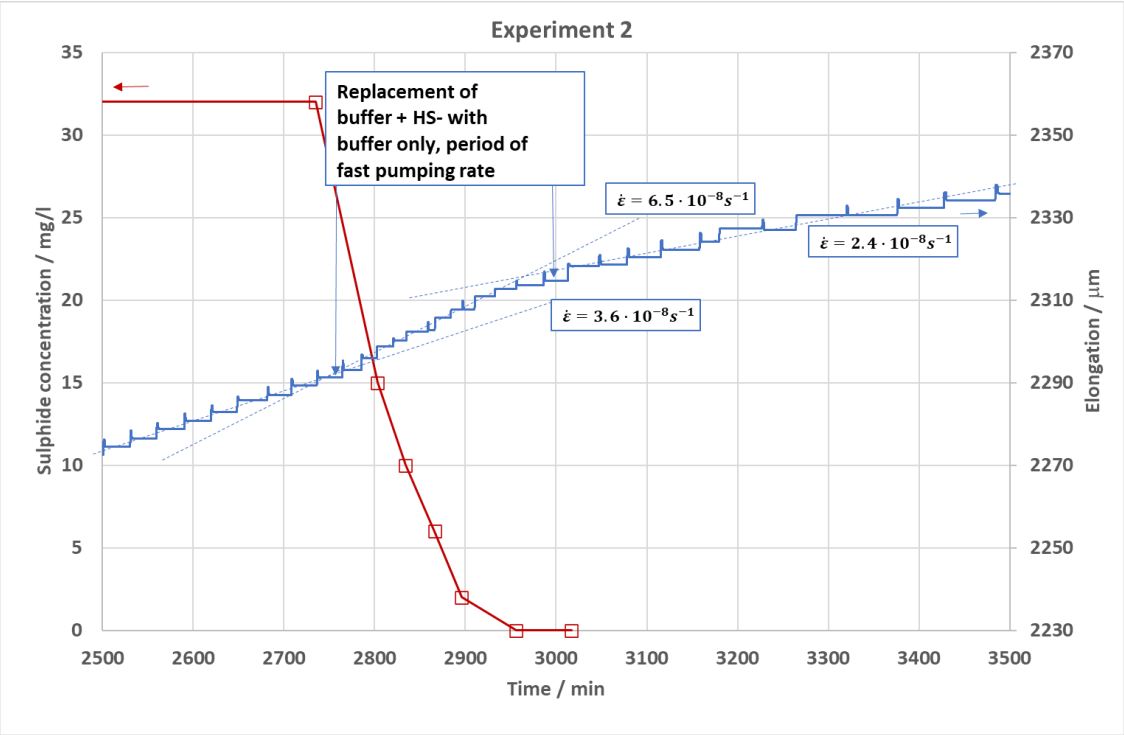

Figure 3-6. *Sulphide concentration and elongation as a function of time.*

During the Experiment 2 the corrosion potential was measured continuously up until the switch of the buffer source, showing again a quite stable potential of about E = -0.65 V_{SHE}. Polarization resistance was measured after that periodically, with corrosion potential measured at the start of each polarization resistance measurement. The result was similar to that reported earlier, in that the anodic branch of the curves showed a decreasing trend, Figure 3-7.

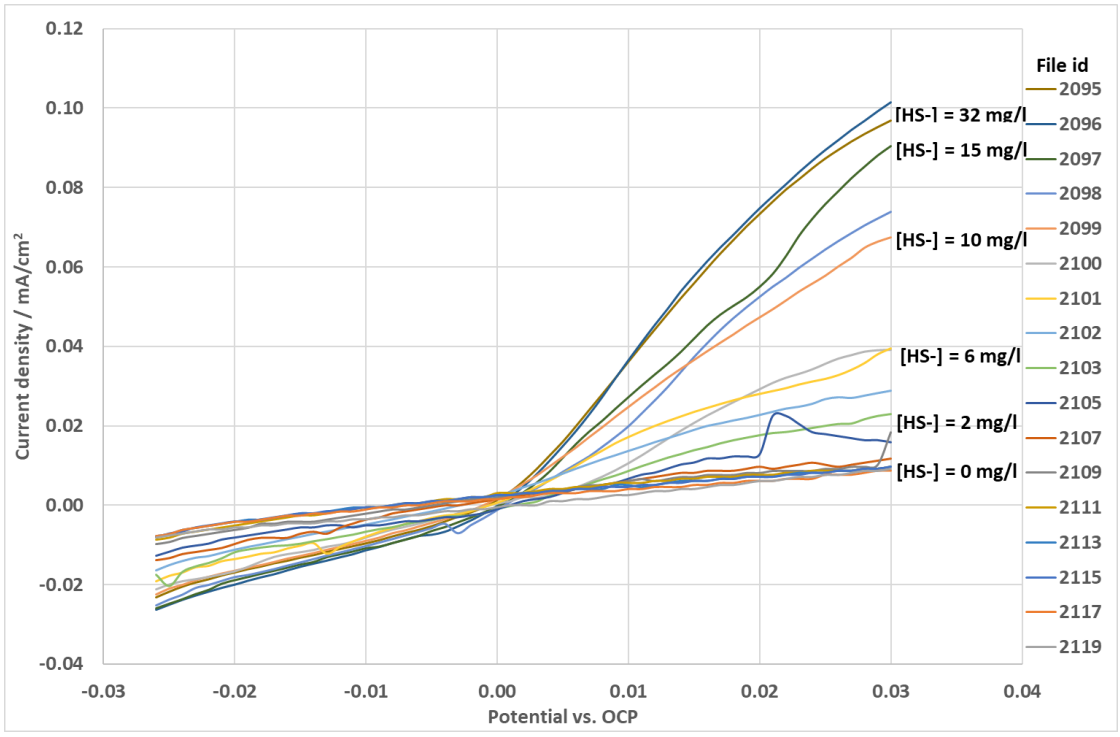

Figure 3-7. *Polarization resistance measurements during the period of switching the buffer source.*

3.3 Experiment 3

The first two tests of the current programme were performed in sulphide by first exposing the Cu-OFP under creep conditions to 32 mg/l (10^{-3} M) sulphide containing buffer (pH = 7.2) for about 48 hrs and then switching the feed into the same buffer without sulphide using a three-way connection in the feedwater line. In both tests with sulphide during the first about 48 hrs, replacing the sulphide containing buffer with the same buffer without sulphide resulted in only a small (about x2) increase in strain rate. In earlier tests, where sulphide was removed by bubbling with N_2, the procedure resulted in a very large (albeit transient) increase in strain rate of up to 100x. This raised the question of the possibility that the bubbling with N_2 could cause the increase in the strain rate. It was decided to perform a test in which there is no sulphide at all, but the test would be run in otherwise similar manner, i.e. follow the change in the sample elongation in the buffer solution up to about 48 hrs and then introduce N_2 bubbling through the solution.

Figure 3-8 shows the stress and elongation and Figure 3-9 the potential and strain rate during the test. The elongation rate (strain rate) clearly increases as the bubbling is started, although only by a factor of about x3 at maximum. The test was continued for another 115 hrs, and the elongation rate is seen to fall back close to the original one towards the end of the test, i.e. the increase in the elongation is of transient nature.

The corrosion potential was about + 0.09 V_{SHE} in the beginning, and slowly decreased to about +0.04 V_{SHE}, towards the end of the first about 48 hrs (no N_2 bubbling). In this period, the potentials were all the time in the stability area of Cu_2O, indicating the presence of an air formed oxide. Note that the air formed oxide was not removed by cathodic cleaning before starting the experiment. The slowly decreasing trend of the corrosion potential indicates that the air formed oxide is slowly reducing to Cu. The start of the bubbling markedly increased the rate of the reduction of the air formed oxide, resulting in a rapid decrease of the corrosion potential, finally stabilizing at about -0.31 to -0.32 V_{SHE}, in the stability area of Cu and about 0.1 V above the hydrogen line (reducing conditions). The strain rate is seen to increase after starting the N_2 bubbling, with a maximum of about 3x, and then slowly decreasing to the same level as before starting the bubbling, i.e. about $3x10^{-9}$ s^{-1}.

Note that there is a small possibility that the dissolved oxygen concentration in the feed water is not zero (in this case, when there is no sulphide), although we have never seen any evidence of that. The water is pumped from the storage vessel (in which there is a continuous N_2 blanket) to the autoclave with a tube pump which has a silicone tube, known to be slightly permeable to oxygen from the surrounding air. However, the remanence time of water in the silicone tube is rather short, so in-leakage of oxygen is not probable. Likewise, there is a small fraction of oxygen in the 5N N_2 that we use (1-3 ppm), and thus bubbling will also bring a small amount of oxygen into the system. Based on the measured potential in the present experiment, this small amount does not seem to have an influence on the potential.

There are two hypotheses for the increase in the strain rate (due to the start of the bubbling) in this case. The first is that the increase is due to the physical effect of bubbling on the specimen, i.e. mechanical force. This seems unlikely since the increase is only about x3 instead of the previously measured (in sulphide containing buffer) up to x100. The other hypothesis is that the increase in strain rate is due to reductive dissolution of the remnants of the air formed oxide. This is considered to be more likely, since the air formed oxide has typically a thickness of a few nanometres, whereas the sulphide film formed due to exposure to sulphide containing water typically has a thickness of several micrometres. Thus, if the strain rate increase is due to reductive dissolution of the surface film, the strain rate increase due to the much thicker sulphide film than the air formed oxide would be expected to be much higher, which is the case here.

To further verify either of the considered hypotheses an additional experiment was performed, in which the air formed oxide was cathodically removed at the start of the exposure.

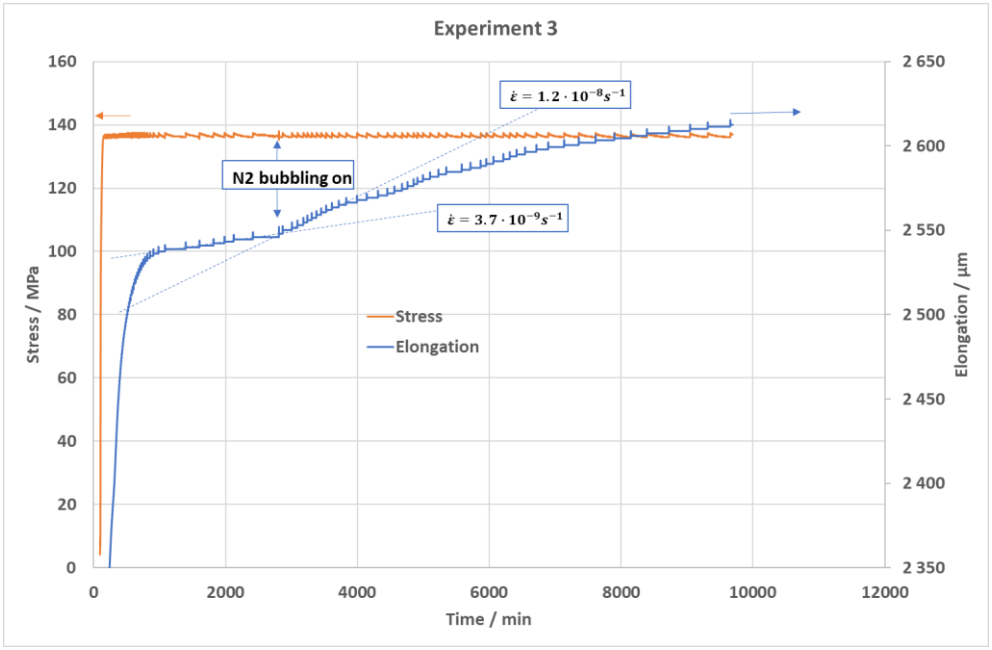

Figure 3-8. *Stress and elongation as a function of time.*

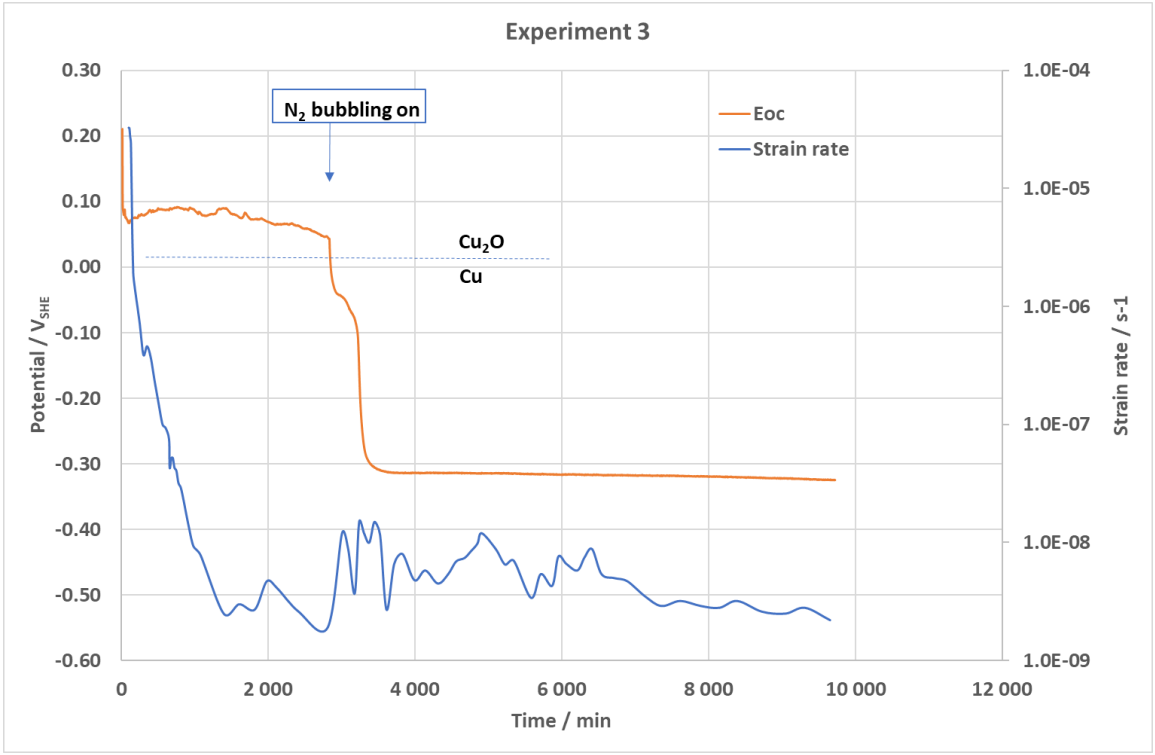

Figure 3-9. *Corrosion potential and strain rate as a function of time.*

3.4 Experiment 4

The cathodic cleaning was performed at -0.6 V_{SHE}, just above the so-called hydrogen line, ensuring that no hydrogen is generated (due to water decomposition) on the surface. Figure 3-10 shows the stress and elongation and Figure 3-11 the potential and strain rate during the test. The elongation rate (strain rate) increased by only by a factor of x1.5 as the N_2 bubbling was started, although the variability of the strain rate is seen to increase somewhat.

The cathodic cleaning was performed just before starting the recording of the corrosion potential. The corrosion potential, after the cathodic cleaning was stopped, remained below the Cu_2O/Cu stability line, i.e. in the stability area of Cu. Figure 3-12 shows a perhaps surprising detail – after the corrosion potential had stabilized after the cathodic cleaning was stopped and the loading was initiated, an increase in the corrosion potential by about 0.15 V was observed. The reason for this is for sure the mechanical loading, but the mechanism of the phenomena remains unclear for the moment. One possibility is that the ends of the slip planes protruding out from the surface have a much higher surface energy and are thus also electrochemically more reactive. Since the corrosion potential still remained in the stability range of Cu, no oxide formation was taking place and thus the test is considered valid from the point of studying a sample without a pre-formed oxide film.

Based on the results from this experiment, if the sample is free from a surface film, the N_2 bubbling causes only a very small increase in the average strain rate (although increase in the variability of the strain rate is observed). This strengthens the hypothesis that the earlier observed (up to x100) increase in the strain rate due to N_2 bubbling is caused by reductive changes in the existing surface film (dissolution of the film or changes in the oxidation state within the film). The mechanism behind the phenomena could involve either injection of vacancies into the base metal or hydrogen egress/ingress, both able to influence the dislocations and thus to cause the observed increase in the strain rate.

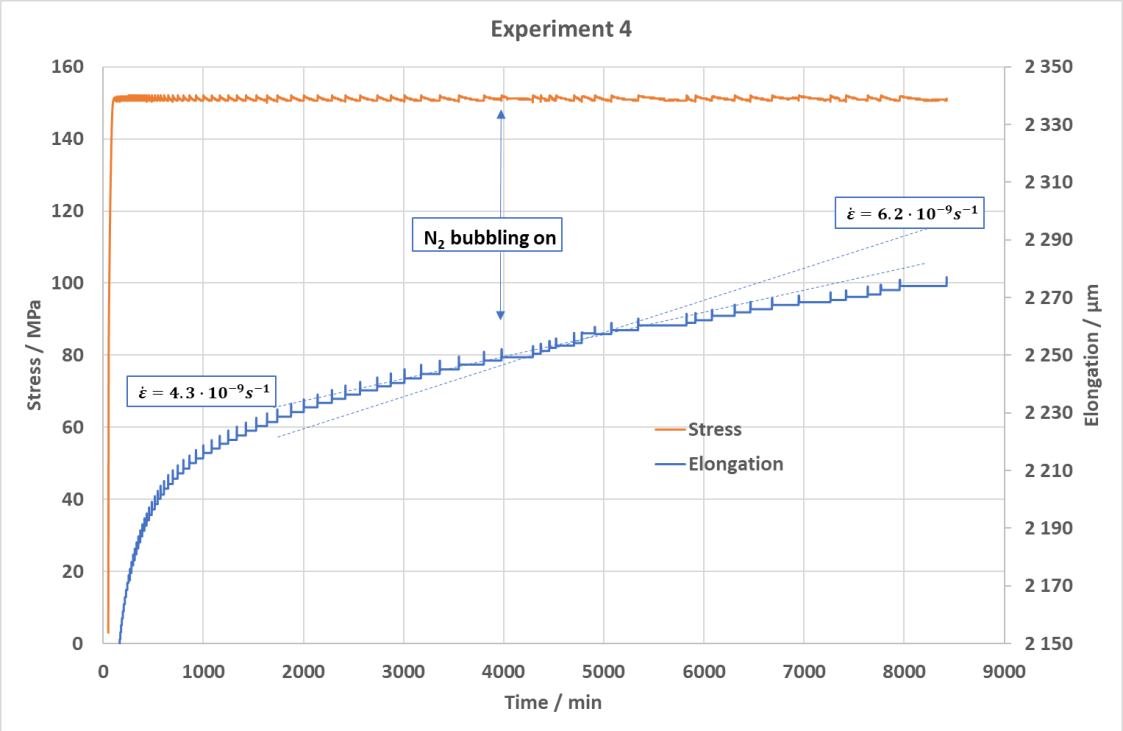

Figure 3-10. *Stress and elongation as a function of time.*

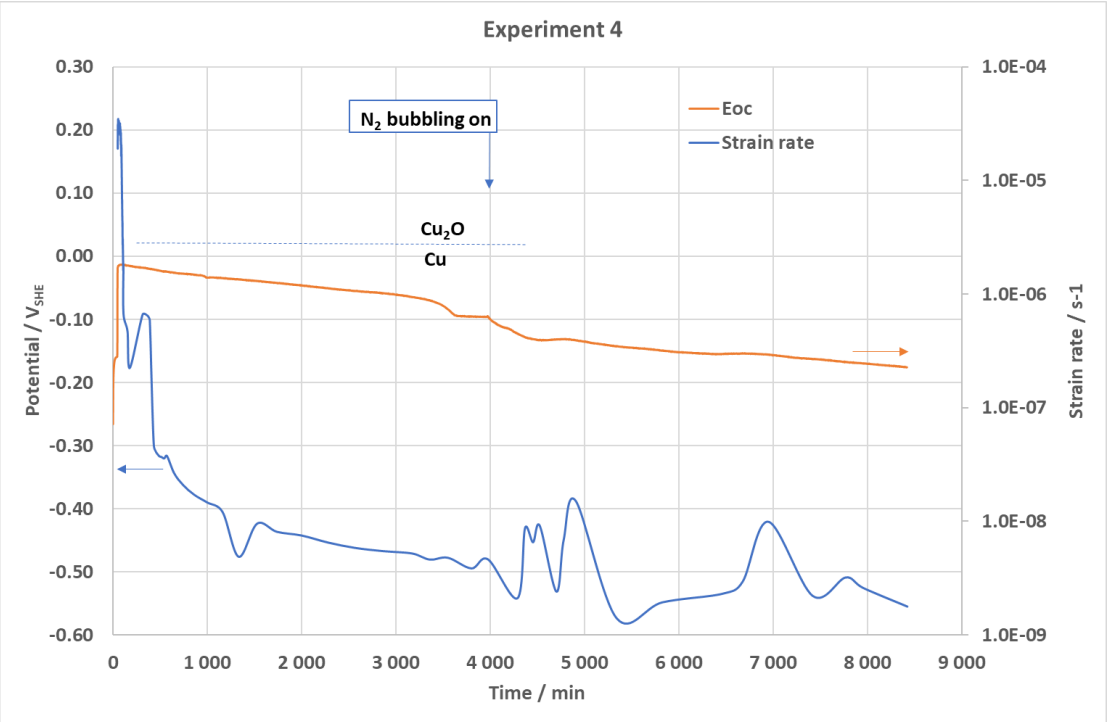

Figure 3-11. *Corrosion potential and strain rate as a function of time.*

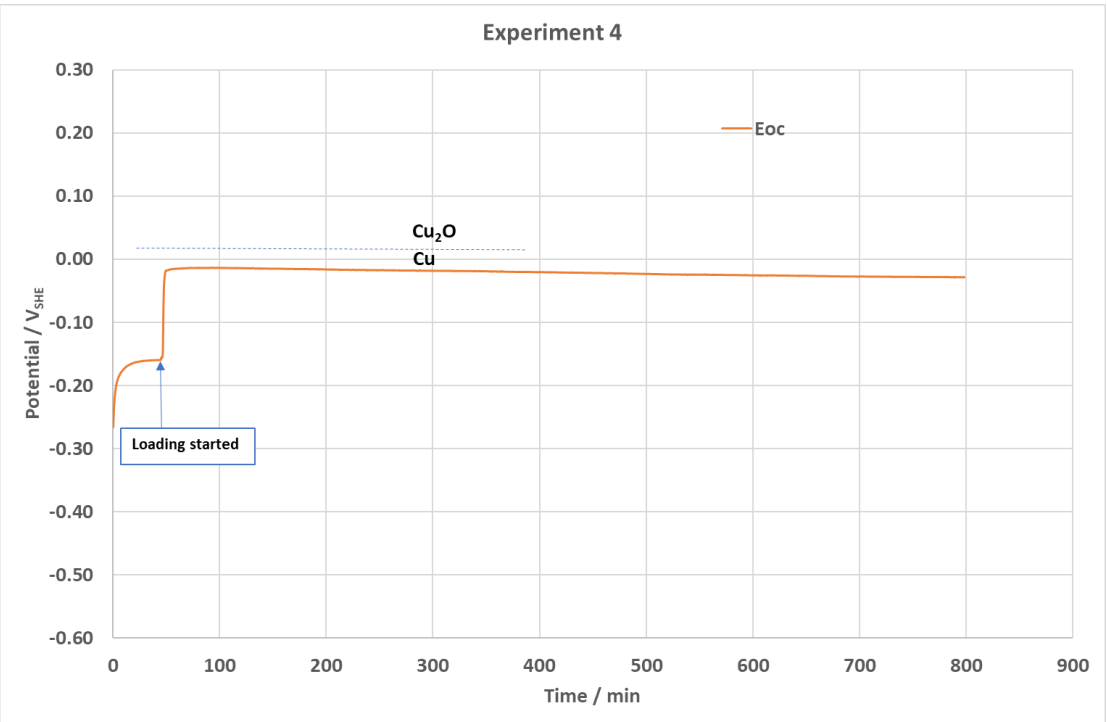

Figure 3-12. *Corrosion potential (detail of Figure 3-11) at the time of loading initiation.*

3.5 Experiment 5

The aim of this test was to verify whether the oxide formation at the metal interface observed in previous tests occurs during the test or afterwards, during the metallographic sample preparation.

Two small (internal volume about 1 l, Figure 3-13) flow-through cells were manufactured from AISI 316 stainless steel. In order to condition the cells, they were connected to the water lines and buffer solution with 10^{-3} M sulphide was directed through them for about 48 hrs. This was done to saturate the cell walls and piping with sulphide. Specimens were not inside the cells during this conditioning phase.

Four coupon samples of Cu-OFP (T58) were prepared with a final polishing made by 1200 # SiC paper. Two coupons were placed inside each cell, supported by PTFE covered wire so that the coupons did not have contact with the cell walls. The buffer solution with 10^{-3} M sulphide was directed through the cells (connected in series as shown in Figure 3-14) for 48 hrs. The sulphide concentration was measured in the beginning, after 24 hrs and at the end to be consistently at 10^{-3} M (measured from the outlet).

At the end of the test, the two cells were isolated with valves, and cell Nr 1 was emptied with N_2-gas, followed by a continuous N_2-flow through the cell for the whole period before transferring the cell to the SEM/FIB-room. The cell Nr 2 was also emptied from the solution with N_2-gas and opened up immediately after that. Both samples from cell Nr 2 were then rinsed with ion pure water and ethanol, dried with blowing air and given to the metallographic lab for preparation of a normal cross-section for SEM-study.

The SEM-sample from cell Nr 2 showed a rather continuous surface film, Figure 3-15, with a thickness of 0.5 to 1 µm. The EDS mapping at one of the location is shown in Figure 3-16. In both cases, there is a continuous line of O at the film-base metal interface, while the S containing film on top seems less continuous. Small traces of both Na and P were also detected, obviously originating from the buffer solution.

The cell Nr 1 was opened in the SEM/FIB-room after about 100 hrs from removing the solution from the cell (during which time the cell was under continuous N_2-blanket). Transfer of one of the coupons from the cell to the SEM/FIB-chamber took about 4 minutes, during which time the coupon was exposed to air.

The SEM-sample from cell Nr 1 showed separate hexagonal crystals on the outer surface, which were rich in S and Cu, Figures 3-17 and 3-18. In addition, Na, P and O were detected, originating from the buffer solution. Note that since the coupon from the cell Nr 1 was not rinsed with ion pure water (and ethanol), the remnants of the buffer solution have dried on the surface during the N_2-gas flow used to dry up the cell internals, thus explaining the Na, P and O findings.

The SEM/FIB cuts through the surface of coupon from cell Nr 1, Figures 3-19 and 3-20, do not show a continuous line of O at the film/base metal interface (two different locations were studied). Some particles on the surface seem to consist of Na, P and O, in line with the findings on the outer surface shown in Figure 3-18. The S and Cu rich layer on the surface is somewhat discontinuous, indicating that the sulphide film is not well adherent (or not well formed).

It should be noted that determining an exact chemical composition based on SEM/FIB analyses only is not easy and that a better understanding of the composition of the details found could be reached by TEM analyses, although at a much higher cost. For the purposes of this work, though, the results gained by SEM/FIB are considered sufficient.

The results strongly indicate that the thin continuous line of oxygen observed at the surface film/base metal interface found in earlier studies and here for the SEM-sample manufactured through the conventional route, is forming during the SEM sample preparation stage and not during the actual exposure. The reason for this could be that the sulphide film is rather porous and not adhering well to the base metal surface, thus offering routes for the oxygen saturated water to ingress into the surface film and all the way to the film/base metal interface during the wet polishing stages of the conventional SEM-sample preparation. Also, the atoms at the metal surface are probably at a higher energy and thus more ready to react with oxygen, if available.

Figure 3-13. *Picture of the flow-through cells, connected to the water and N_2-gas tubing.*

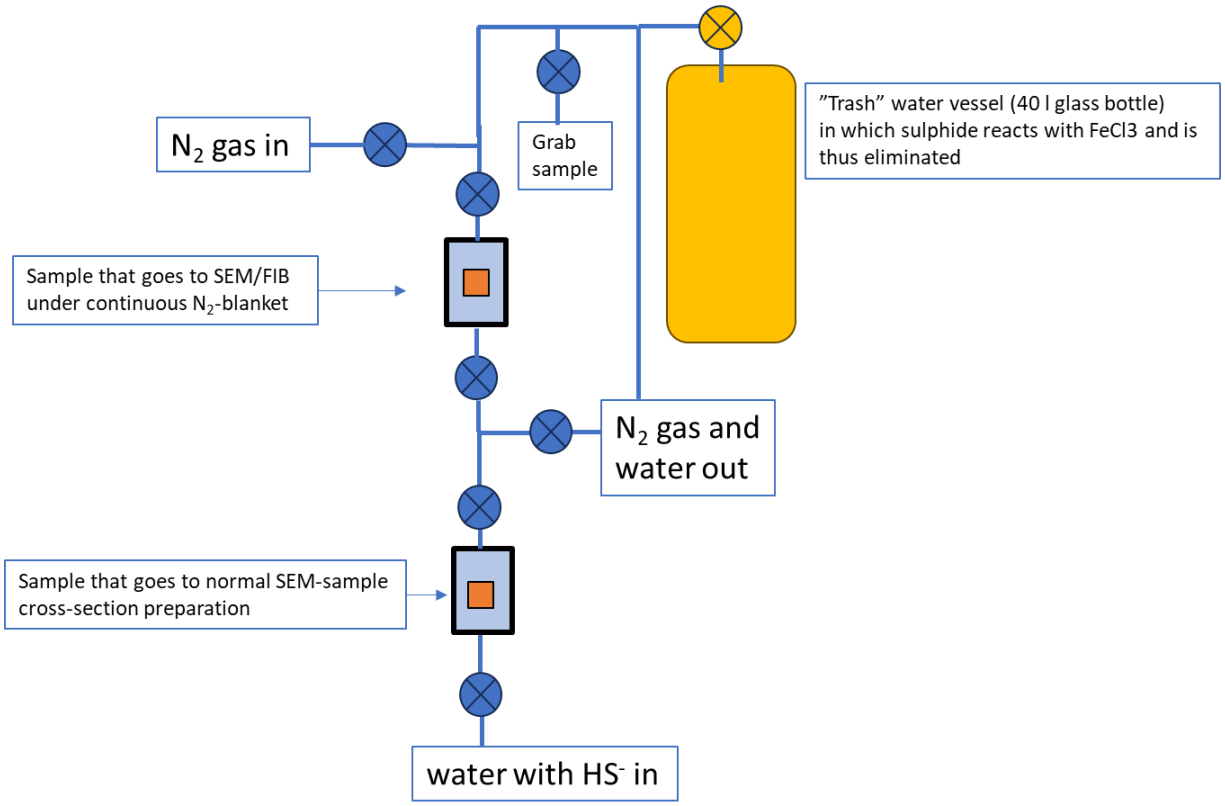

Figure 3-14. *Scheme for the flow-through cell arrangement for the test.*

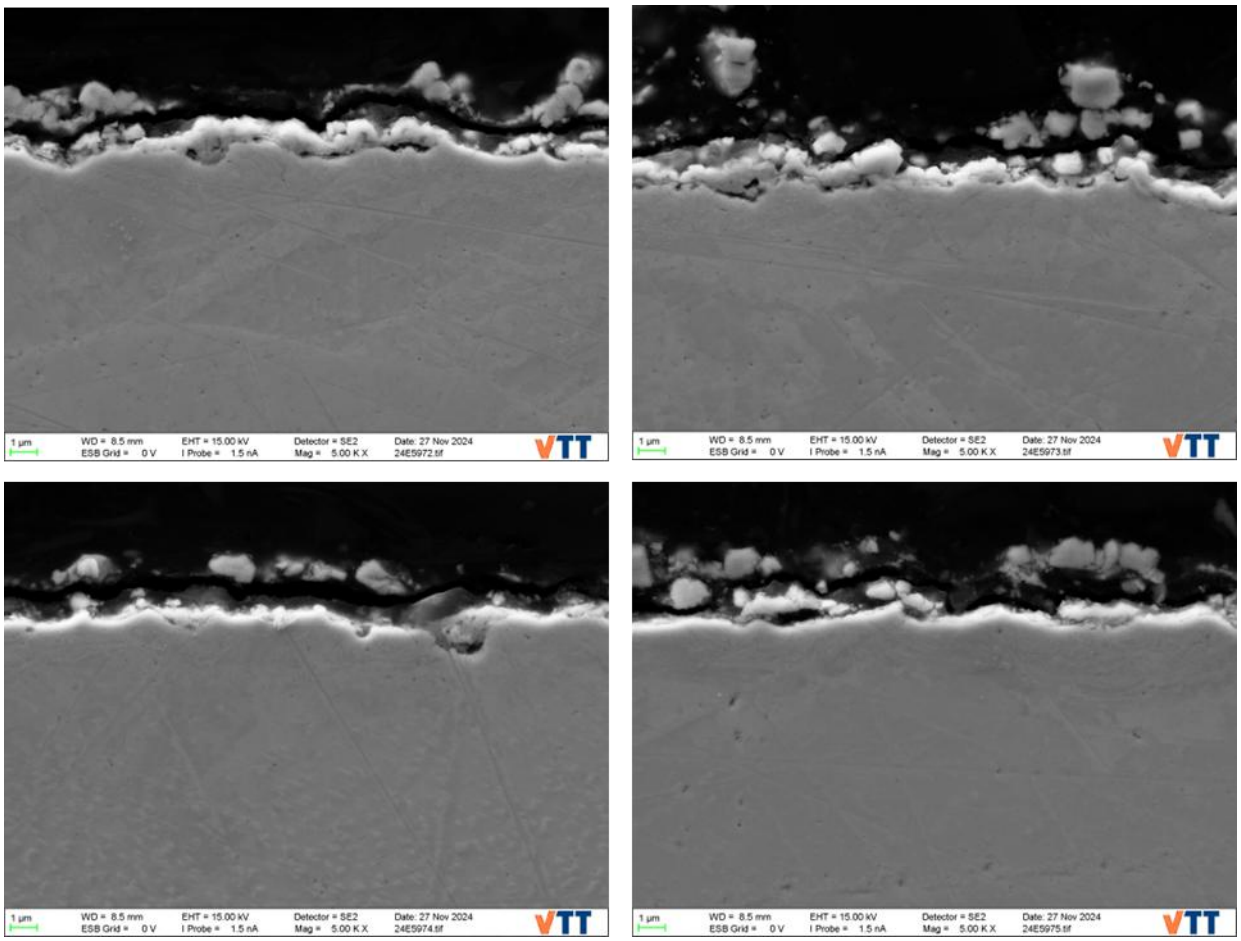

Figure 3-15. *SEM cross-section of the sample from cell Nr 2, four different locations.*

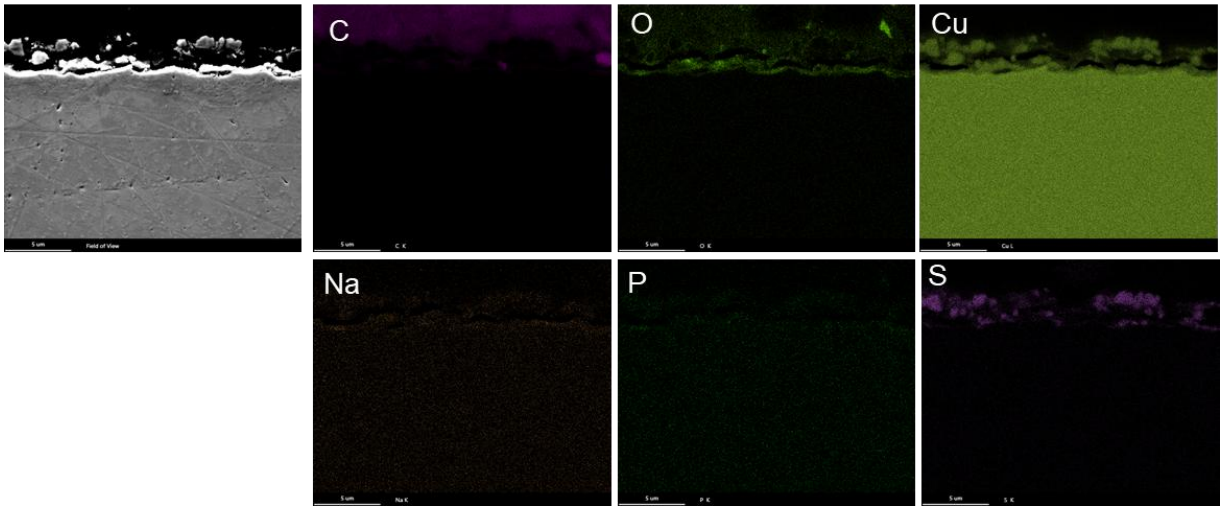

Figure 3-16. *EDS map of the sample from the cell Nr 2*

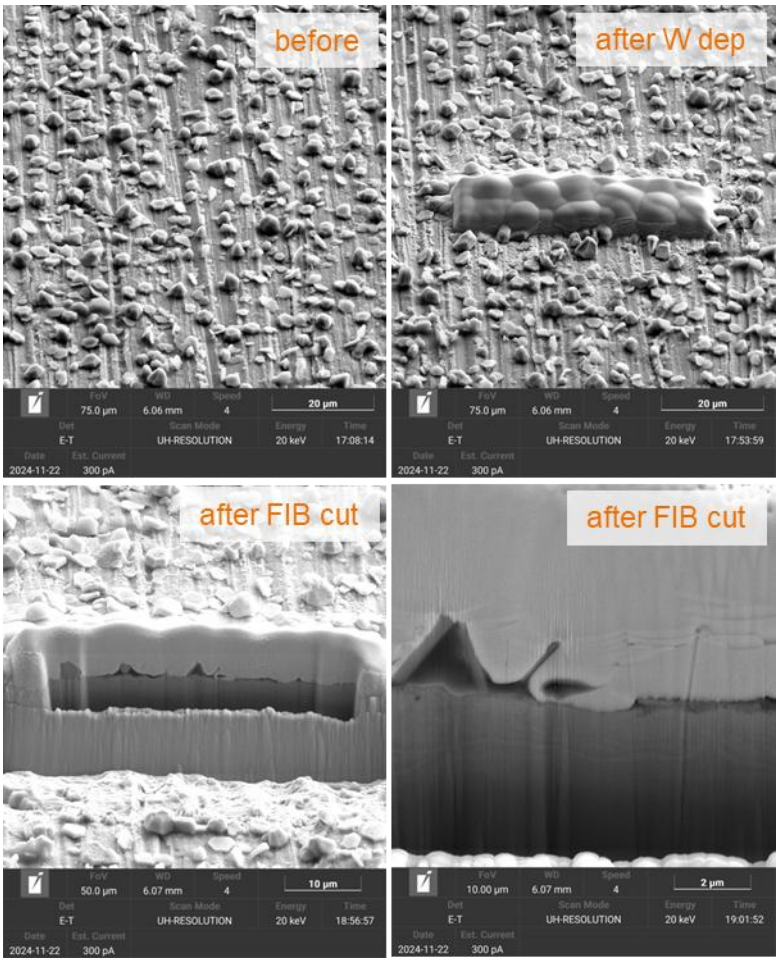

Figure 3-17. *The coupon from cell Nr 1 before and after the FIB cut.*

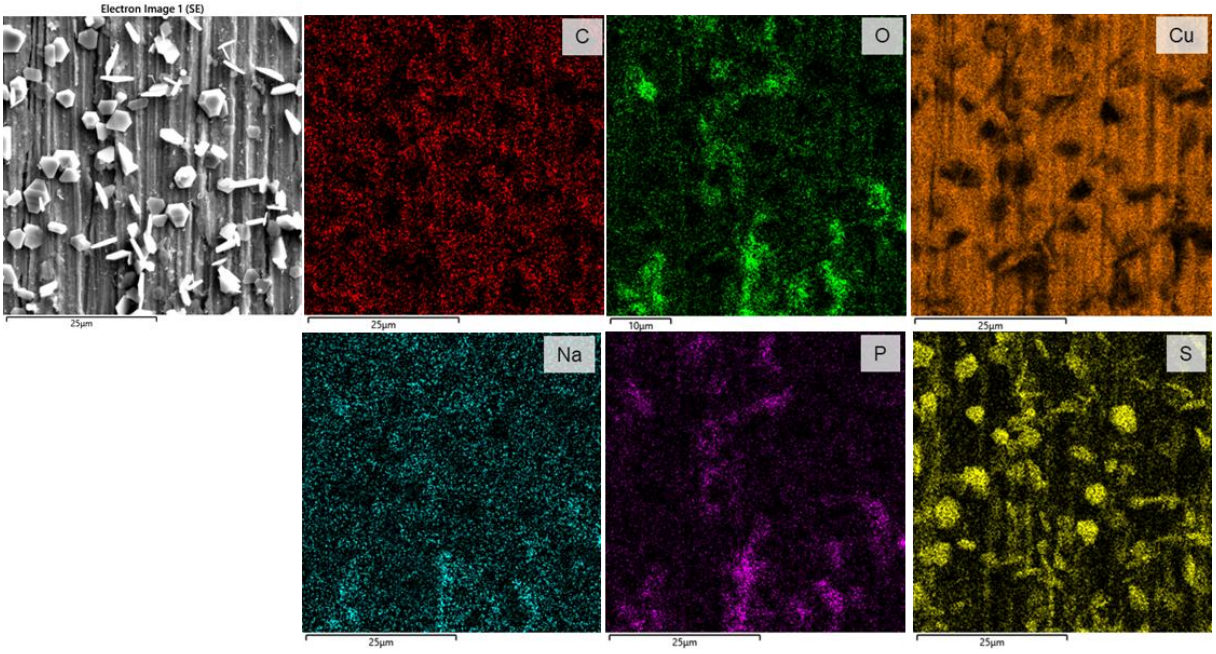

Figure 3-18. *EDS map of the outer surface of coupon from cell Nr 1.*

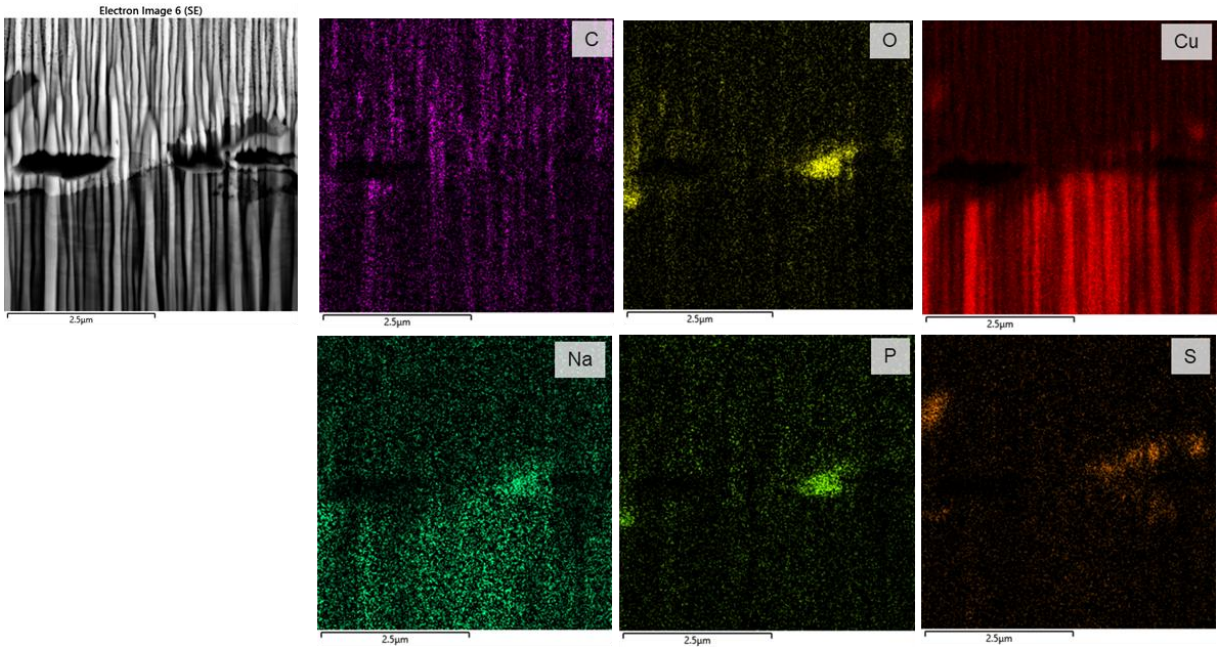

Figure 3-19. *EDS map of the FIB cut of coupon from cell Nr 1, location 1.*

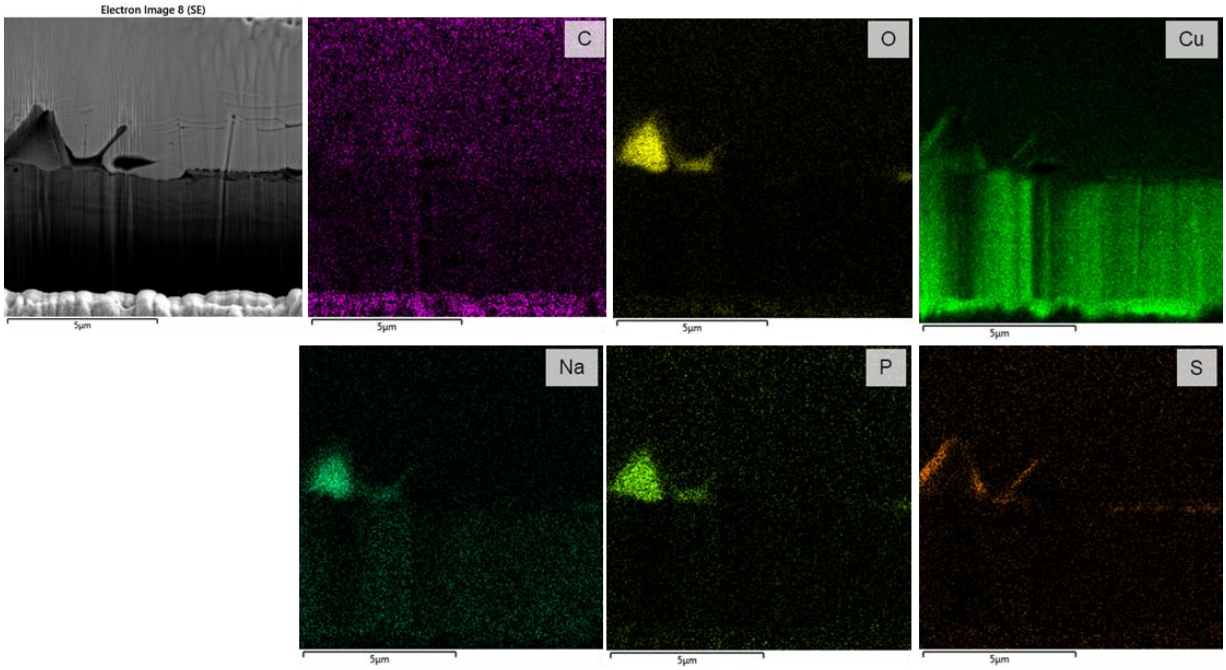

Figure 3-20. *EDS map of the FIB cut of coupon from cell Nr 1, location 2.*

3.6 Experiment 6

The aim of this test was to verify whether the oxide formation and reduction cycle produces an increase in the creep rate of Cu-OFP.

A creep test was prepared with the same specimen design as before. After installing the specimen, the pressure vessel was filled with the buffer solution, closed and purged with 5N N2-gas for several hours. Corrosion potential of the specimen at the end of the purging period was -0.07 VSHE, clearly in the stability area of pure copper (red dot in Figure 3-21). The specimen was then polarized cathodically to -0.4 VSHE for 15 minutes to remove any remnants of the air formed oxide, after which the SSRT loading was initiated.

During the creep test, three different anodic potentials were used, +0.1 VSHE, +0.35 VSHE and +0.45 VSHE. The first potential is in the Cu2O stability area, while the other two are in the Cu(OH)2 stability area (see Figure 3-21). The time allotted for the anodic film formation was 30 minutes in all cases, followed by a cathodic reduction at -0.4 VSHE for 15 minutes. The cathodic potential of -0.4 VSHE was chosen to avoid hydrogen generation at the sample surface (due to water reduction). The N2 bubbling was stopped at t = 1400 min and kept off for the rest of the test period.

Figures 3-22 and 3-23 show the stress and elongation as a function of time. No correlation of oxide film formation/reduction with the creep rate was observed. Stopping of the N2-bubbling at t = 1400 min had no effect on the creep rate, immediately or during the following anodic/cathodic cycles. A clear increase in strain rate was observed at about t = 7400 min, roughly with a factor of x5. This transient lasted for about 33 hrs and is proposed to have been caused by some anomaly in the material. An anodic/cathodic polarization cycle was performed approximately 5 hrs prior to the initiation of the transient. Given the 5-hour delay and the absence of repeatability, it is considered unlikely that the transient's appearance was caused by the polarization cycle.

Note that the test was still continued for another about 5 days (up to about 19 000 minutes) with two additional anodic/cathodic cycles (+0.45 VSHE 30 min + -0.4 VSHE 15 min). No effect of these polarizations was observed on the creep rate.

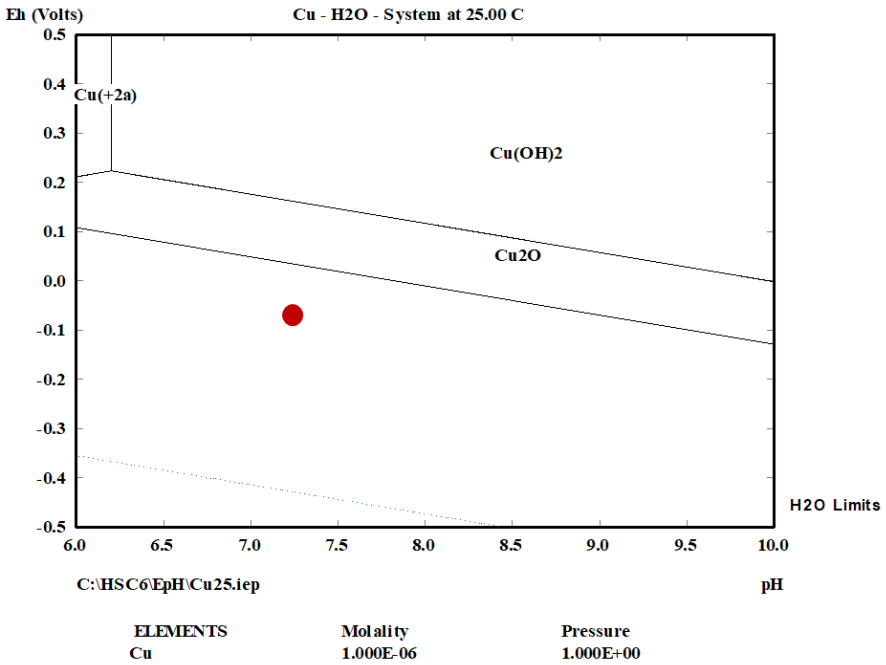

Figure 3-21. *Pourbaix-diagram of Cu at T = 25°C (calculated with Metso Outotec Ltd HSC Chemistry 6.0 software). The red dot shows the corrosion potential of the specimen after purging the water with 5N N_2 gas.*

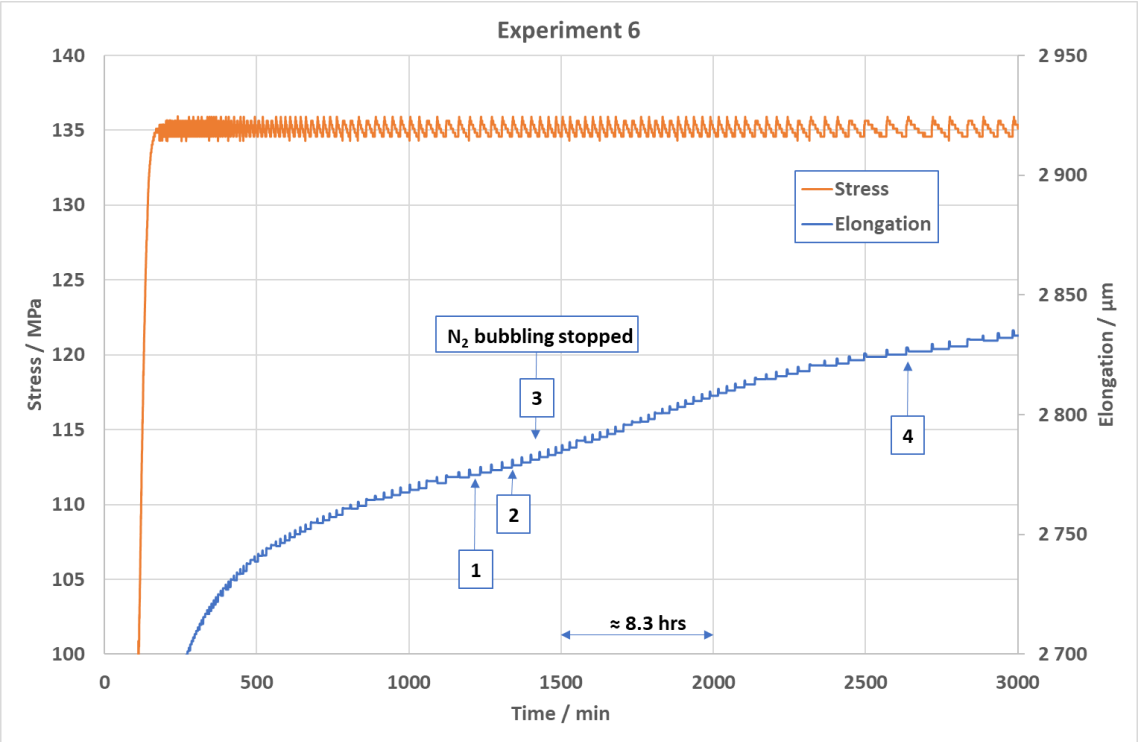

Figure 3-22. *Stress and elongation as a function of time for the first 3000 minutes (50 hrs). 1: +0.1 V_{SHE} for 30 min, followed by -0.4 V_{SHE} for 15 min, 2: +0.35 V_{SHE} for 30 min, followed by -0.4 V_{SHE} for 15 min, 3: +0.35 V_{SHE} for 30 min, followed by -0.4 V_{SHE} for 15 min, 4: +0.45 V_{SHE} for 30 min, followed by -0.4 V_{SHE} for 15 min.*

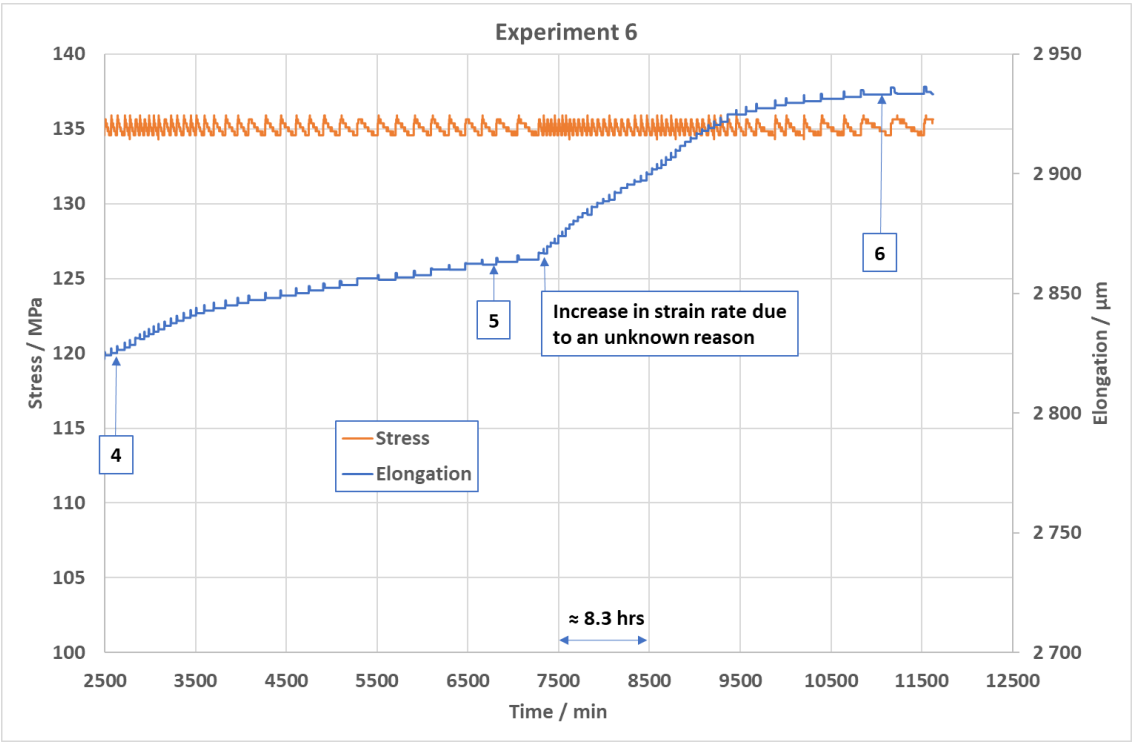

Figure 3-23. *Stress and elongation as a function of time up to 12500 minutes (208 hrs). 4: +0.45 V_{SHE} for 30 min, followed by -0.4 V_{SHE} for 15 min, 5: +0.45 V_{SHE} for 30 min, followed by -0.4 V_{SHE} for 15 min, 6: +0.45 V_{SHE} for 30 min, followed by -0.4 V_{SHE} for 15 min.*

The thickness of the films formed during the anodic polarizations was estimated based on the charge spent in the cathodic reduction process. Plots illustrating the three different anodic/cathodic polarization cycles are shown in Figure 3-24. The film thicknesses estimated through calculations were 0.12 µm, 0.25 µm and 0.50 µm for the anodic potentials of +0.1 V_{SHE}, +0.35 V_{SHE} and +0.45 V_{SHE}, respectively, thus far thicker than the few nm expected for the air formed oxide.

Based on the work described above, electrochemical reduction of an anodic film formed in the buffer solution without sulphide, i.e. a copper oxide/hydroxide, does not cause a change in the creep rate, with or without having N_2-bubbling on.

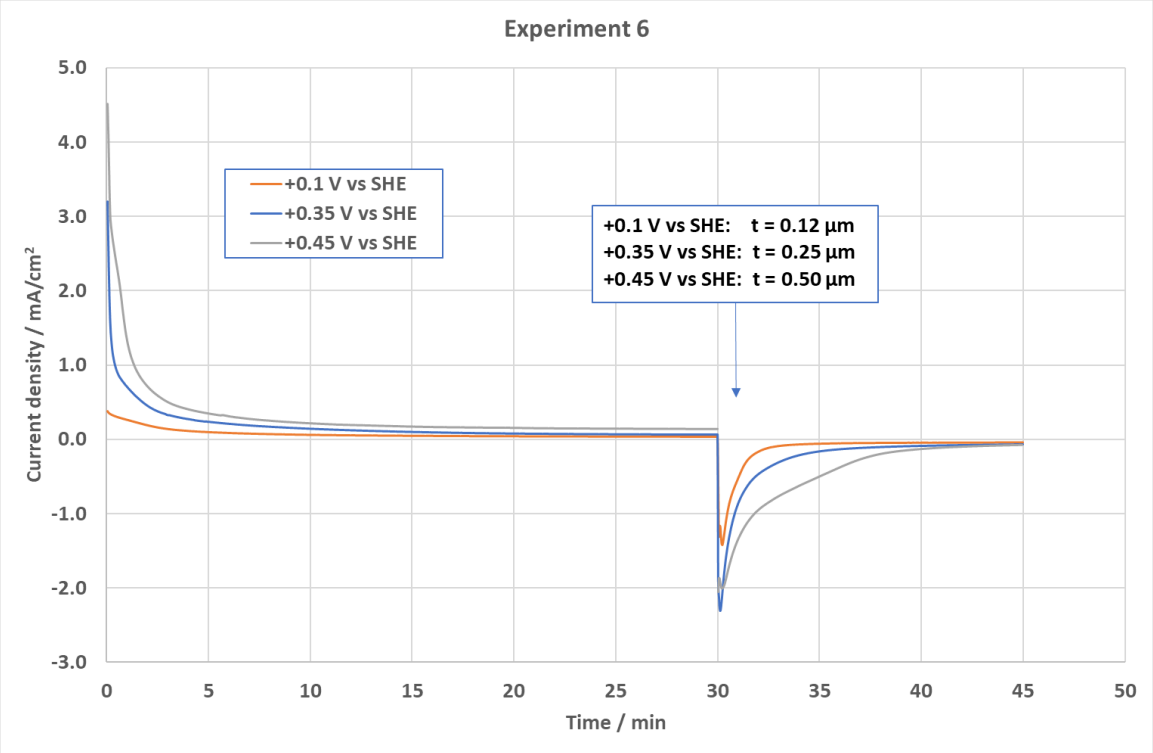

Figure 3-24. *Current density as a function of time for the three different anodic potentials used. The ingress shows the oxide film thicknesses (in µm) calculated from the charge spent in the reduction of the films.*

3.7 Experiment 7 – 0 hrs N_2 bubbling

A series of experiments was performed to produce specimens for Hydrogen Melt Extraction (HME) measurements of the hydrogen concentration in the specimens. The experiments were stopped at times targeted to 0, 2, 4, and 8 hrs from stopping the N_2-bubbling. All experiments were started by exposing the specimen under the same creep conditions as in the previous experiments, i.e. by loading the specimen to 135 MPa in sulphide (32 mg/l) containing buffer solution for about 48 hrs before starting the N_2-bubbling.

The stress and elongation as a function of time for Experiment 7 (Test 1 for H_2) is shown in Figure 3-25, and the corrosion potential and [HS^-] in Figure 3-26. This experiment was stopped just before the N_2-bubbling, thus producing a reference "0 hrs" sample for HME. The average strain rate towards the end of the test was estimated at $\dot{\varepsilon} = 1.6*10^{-8}$ s^{-1}. Note in Figure 3-26 that the potential shows some irregularities, indicating possible problems with the reference electrode. However, since the sulphide concentration was measured consistently at 32 mg/l, the experiment is considered valid. After the test the reference electrode was serviced by changing the electrolyte (KCl) inside the electrode.

After terminating the test, the specimen was immediately removed from the autoclave and the sulphide film on the gauge length was removed by #220 SiC-paper. The gauge length was cut in two pieces, which were washed by ion pure water, rinsed with ethanol and gently dried by warm air (T < 40°C), after which the two samples were placed in a freezer (at -18°C) to wait for the HME analysis. The time from opening up the autoclave to the freezer was slightly below 20 minutes.

The HME showed a hydrogen content of 2.5 ppm. Reference sample showed a hydrogen concentration of 3.4 ppm. However, the reference sample was cut by hand sawing, had a more rugged surface and was much thicker than the gauge length.

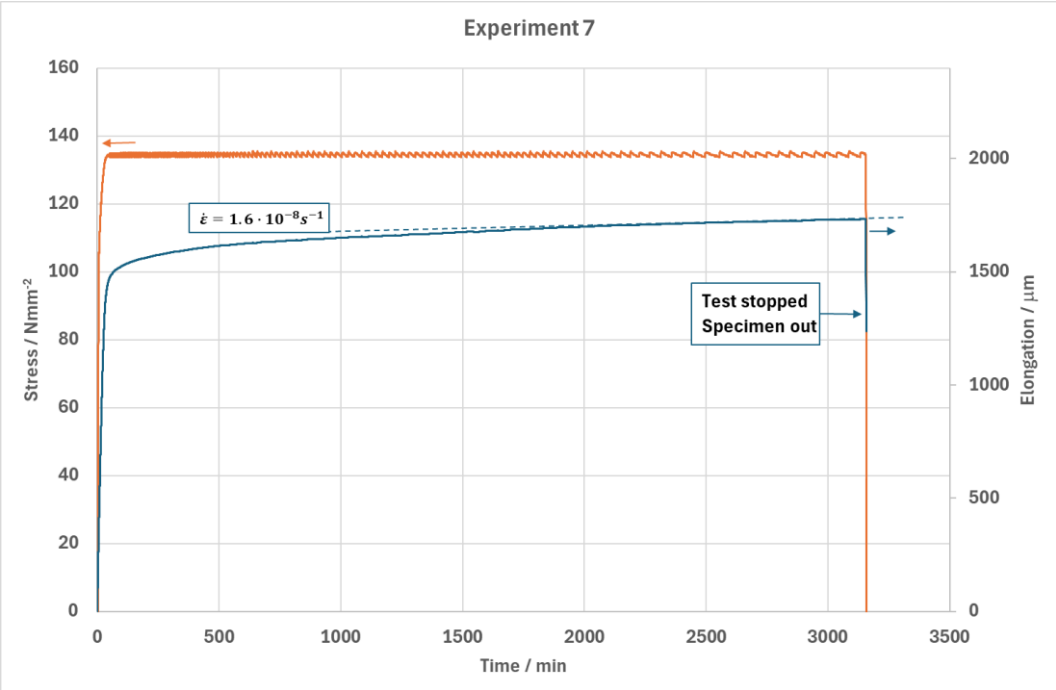

Figure 3-25. *Stress and elongation as a function of time, Test 1 for H.*

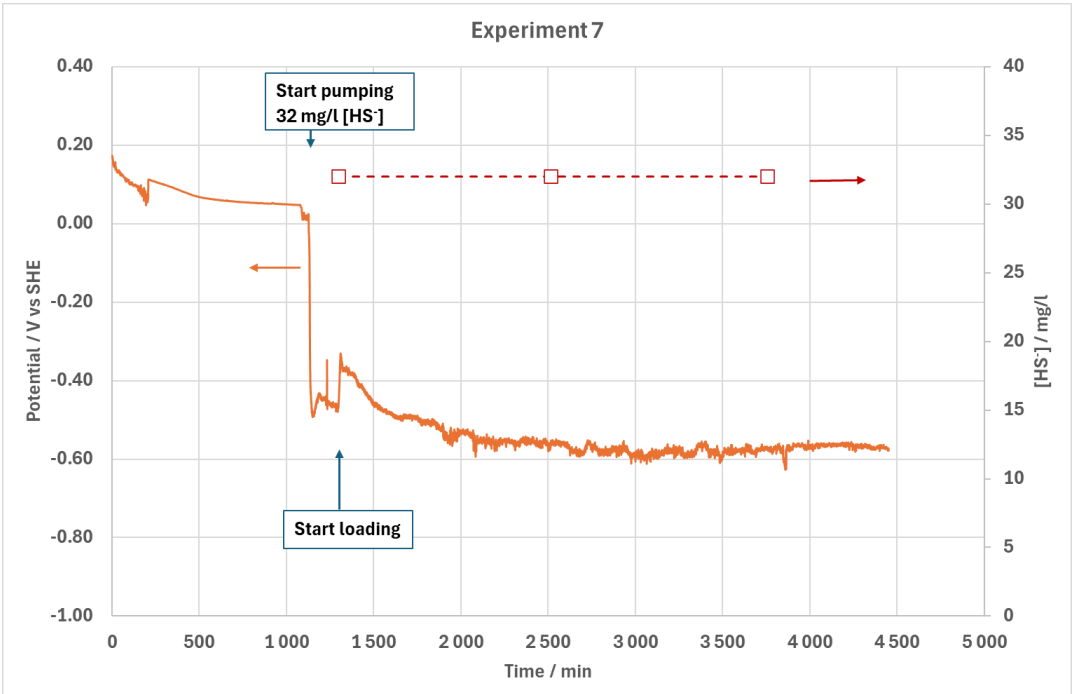

Figure 3-26. *Corrosion potential and [HS$^-$] as a function of time, Test 1 for H_2. Note that the time here is from the start of the experiment, while the time in Figure 3-26 is from the start of the loading.*

3.8 Experiment 8 – 1.7 hrs N_2 bubbling

The stress and elongation as a function of time for Test 2 for H_2 is shown in Figure 3-27, showing an average strain rate towards the end of the test at about $\dot{\varepsilon} = 6*10^{-8}$ s^{-1}. After starting the N_2-bubbling, an almost immediate increase in the strain rate followed, see Figure 3-28, first at about $\dot{\varepsilon} = 2.9*10^{-6}$ s^{-1} and then slowing down to about $\dot{\varepsilon} = 6.8*10^{-7}$ s^{-1}. The former indicates an increase in the strain rate by about x48 and the latter by about x11.

Figure 3-29 shows the corrosion potential and [HS^-] as a function of time. Based on the data the reference electrode servicing done after the previous experiment was unfortunately not effective, and thus the corrosion potential values are considered unreliable. However, since the sulphide measurements showed consistently the targeted value, the test is considered valid. The HME showed a hydrogen content of 3.2 ppm. After this experiment, the reference electrode was again serviced, this time changing also the AgCl-coated Ag-pin and the porous plug in addition to the KCl-electrolyte inside the reference electrode.

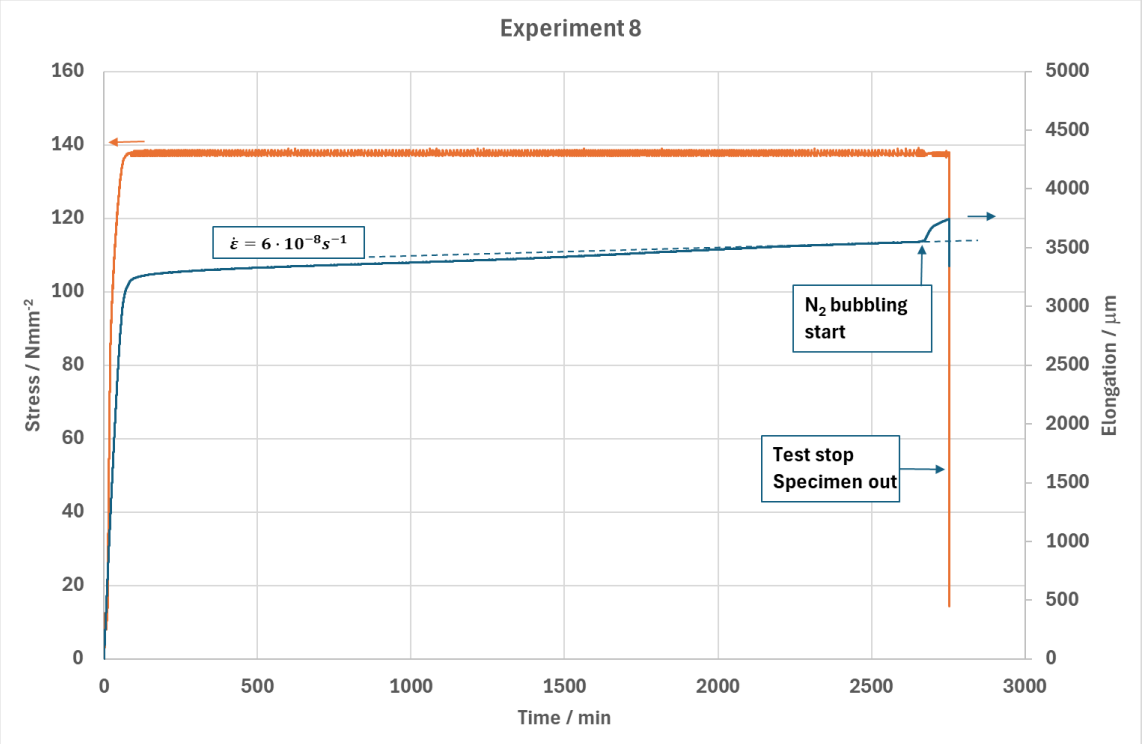

Figure 3-27. *Stress and elongation as a function of time, Test 2 for H_2.*

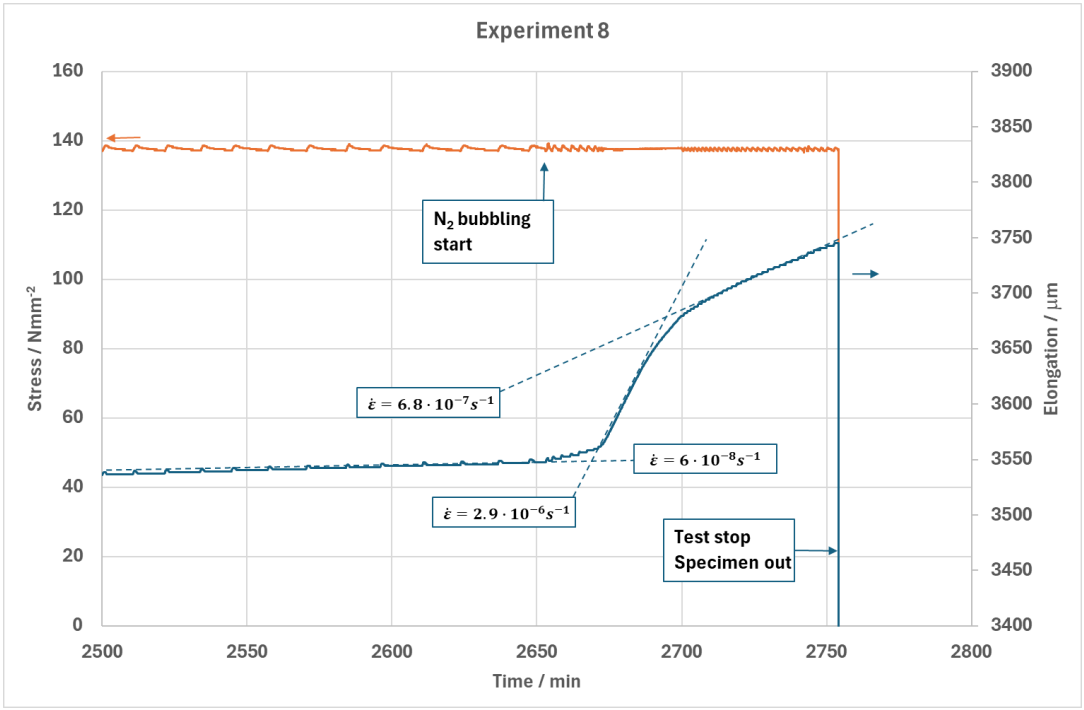

Figure 3-28. *A detail of data shown in Figure 3-28 (time period from 2500 to 2800 min), showing the effect of N_2-bubbling more clearly.*

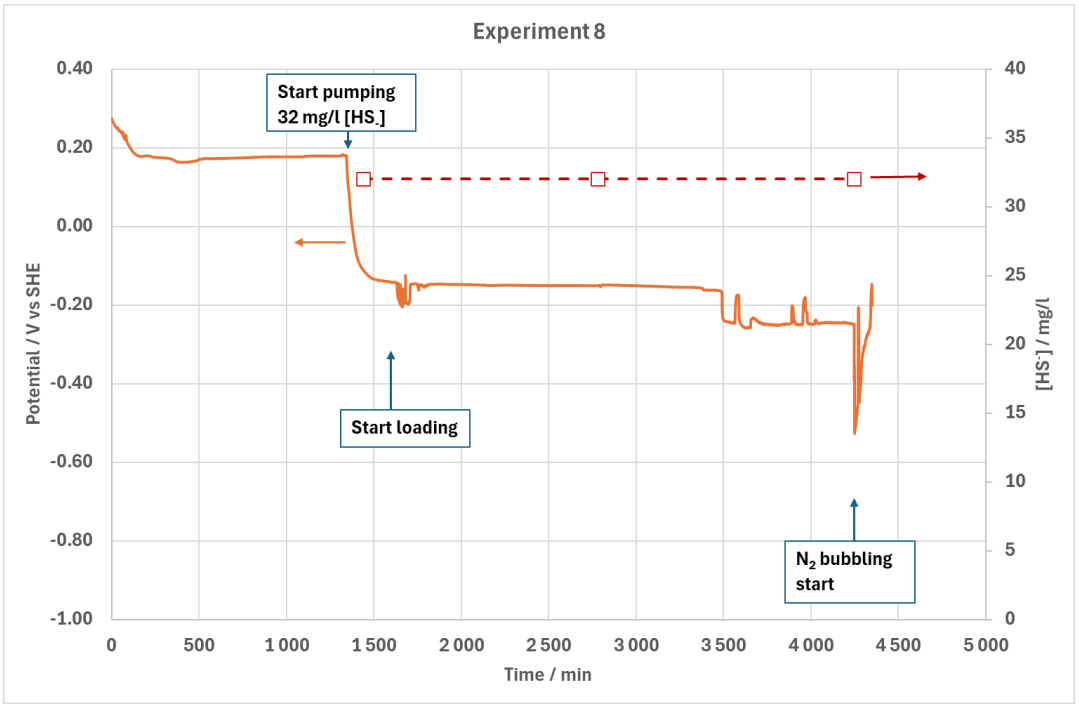

Figure 3-29. *Corrosion potential and [HS^-] as a function of time, Test 2 for H_2. Note that the time here is from the start of the experiment, while the time in Figure 3-28 and Figure 3-29 is from the start of the loading.*

3.9 Experiment 9 – 4.0 hrs N_2 bubbling

The stress and elongation as a function of time for Test 3 for H_2 is shown in Figure 3-30. The average strain rate towards the end of the test at about $\dot{\varepsilon} = 6.5\times10^{-9}$ s^{-1}. After starting the N_2-bubbling, no effect on the strain rate could be discerned, Figure 3-31. This is suggested to result from the bubbling rate being set unintentionally at a rate clearly more vigorous (at least ten times, i.e. > 10 l/hr) than in the previous tests.

Figure 3-32 shows the corrosion potential and [HS^-] concentration as a function of time. Based on the data the reference electrode servicing was effective – some irregularities could still be seen in the beginning part of the test, after which the potential value stabilized into the expected range.

In this test, in addition to the creep specimen, a separate coupon specimen of the same Cu-OFP batch was installed. When preparing for starting the N_2 bubbling, the coupon was connected as the working electrode, in order not to disturb the creep specimen electrochemical equilibrium with the following LPR-measurements. The potential of the creep specimen during the N_2-bubbling was followed intermittently by measuring it with a hand-held meter.

After starting the N_2-bubbling the [HS^-] decreased rapidly (red squares), Figure 3-32, reaching zero within about 2 hrs. The potential of the creep specimen increased during the N_2-bubbling (black circles) with an average rate of 0.54 mV/min. This is very close to the value measured in the experiment where the sulphide was removed from the buffer solution by replacing the water with buffer solution without sulphide, i.e. 0.52 mV/min (see Discussion section below). This strengthens the hypothesis that the rate of increase in the potential during the sulphide removal stage is a key parameter in determining the magnitude of the effect on the creep rate.

The LPR results are shown in Figure 3-33. First, three consecutive runs were performed before starting the N_2 bubbling to act as a reference, showing a highly repeatable result. After that the N_2 bubbling was started, and a series of linear polarization resistance (LPR) measurements was initiated. The first three LPR runs at t = 25, 36 and 48 min showed a clearly higher current density at the anodic branch than the reference runs, indicating an electrochemical activation of the surface. After this, the current density at the anodic branch continued to decrease as a function of time with a diminishing rate, until after about 120 min (2 hrs) no further change was noted, indicating the [HS^-] reaching zero. This is in line with the grab sample analysis of the [HS^-], also showing [HS^-] = 0 mg/l at about 2 hrs from initiating N_2-bubbling.

The HME showed a hydrogen content of 9.6 ppm.

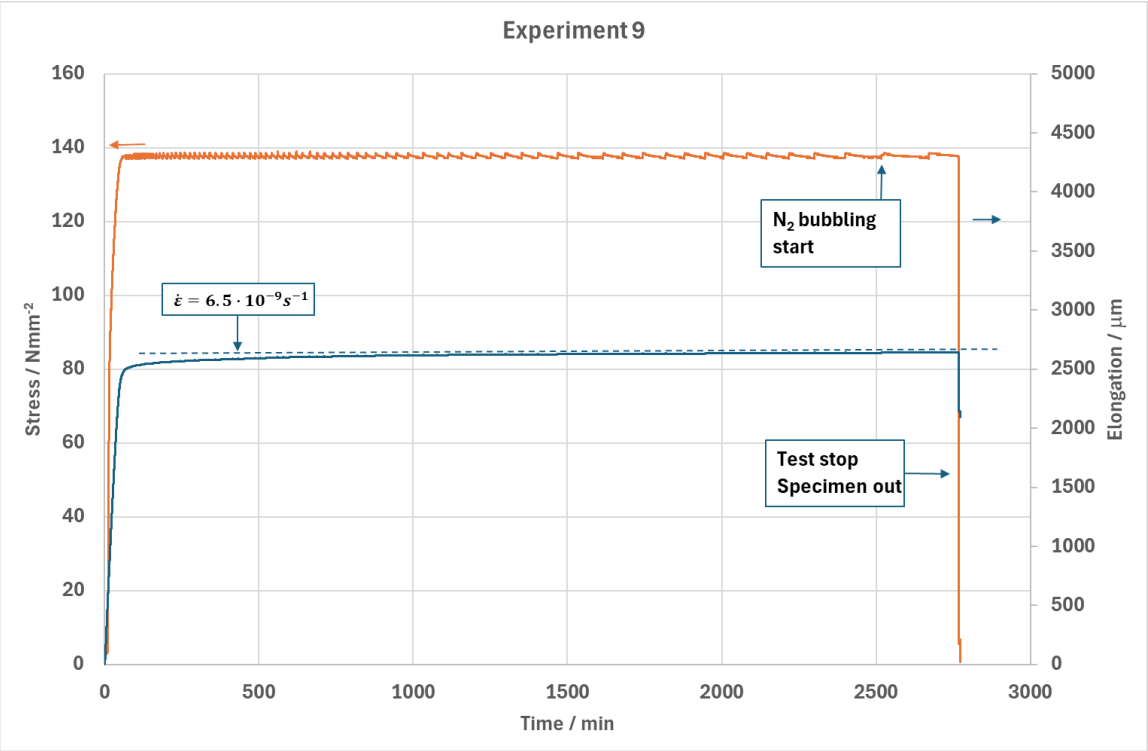

Figure 3-30. *Stress and elongation as a function of time, Test 3 for H_2.*

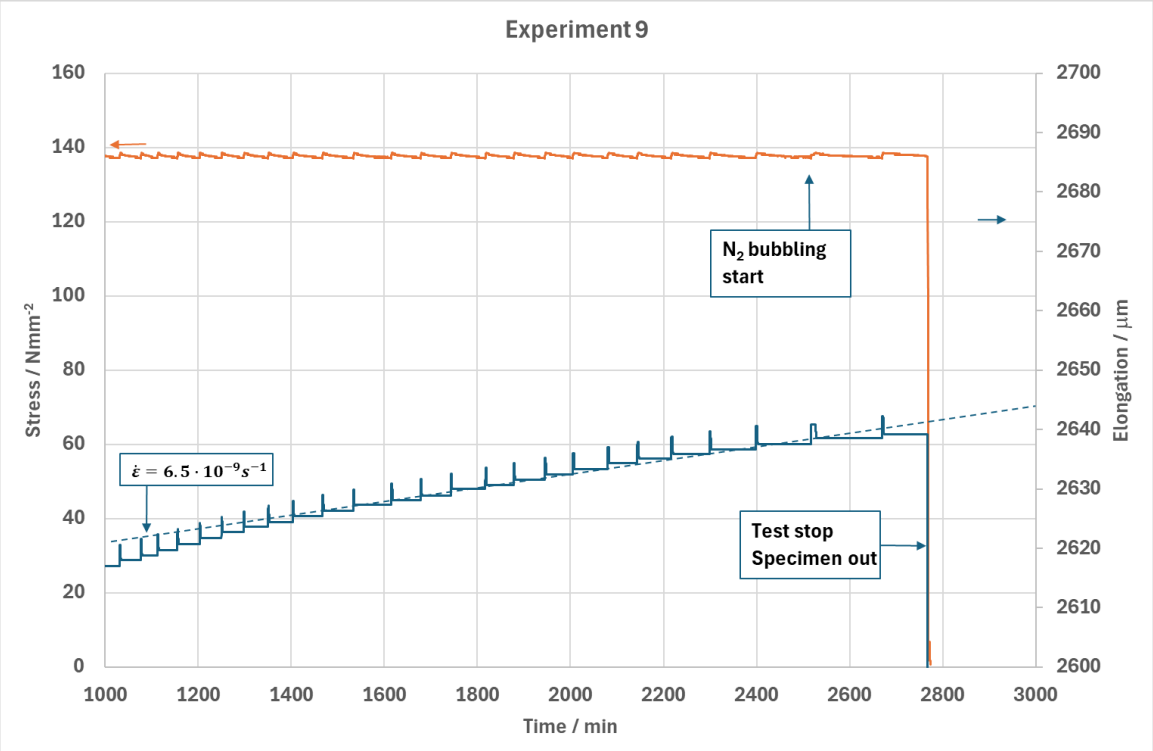

Figure 3-31. *A detail of data shown in Figure 3-31 (time period from 1000 to 3000 min), showing more clearly that starting the N_2-bubbling had no effect on the strain rate.*

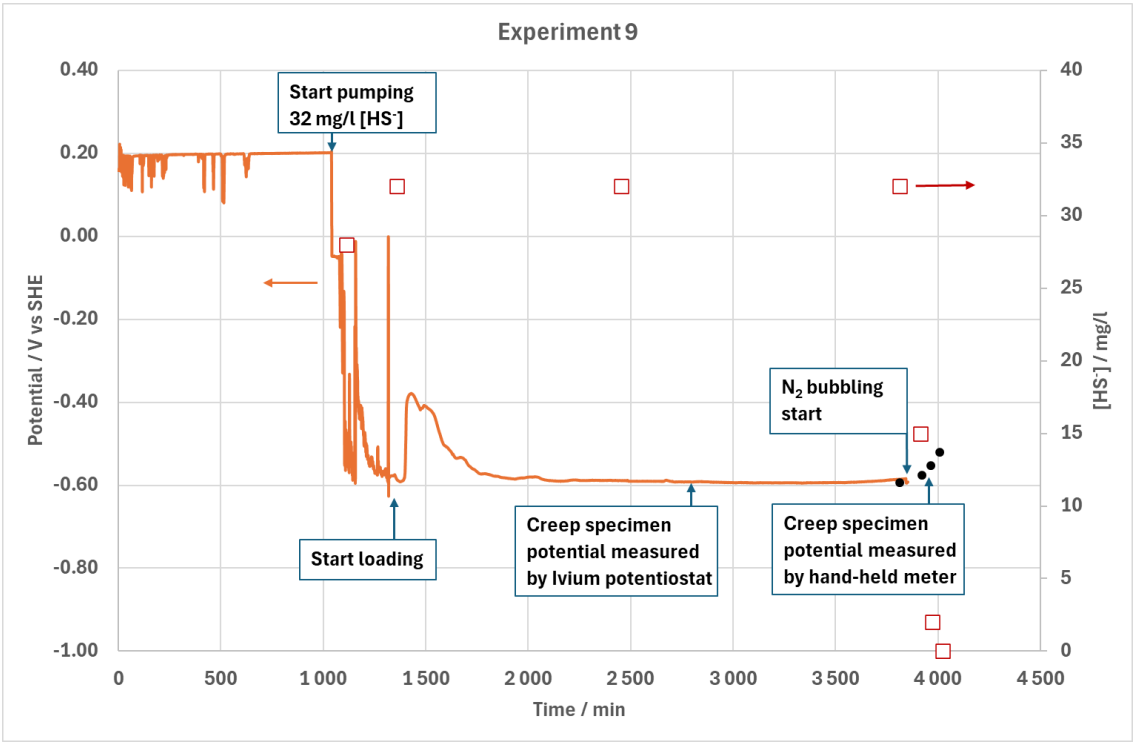

Figure 3-32. *Corrosion potential and [HS-] as a function of time, Test 3 for H_2. Note that the time here is from the start of the experiment, while the time in Figure 3-31 is from the start of the loading. Red squares depict the [HS-] measured from grab samples and the black circles the corrosion potential of the creep specimen measured by a hand-held meter.*

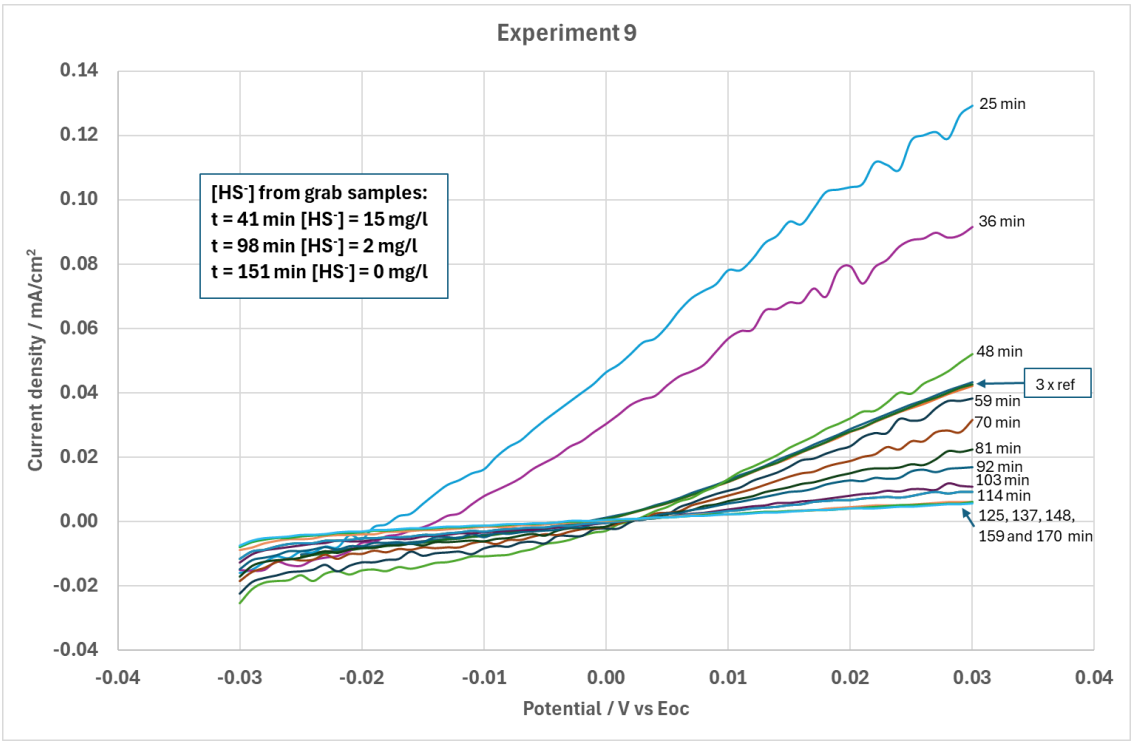

Figure 3-33. *The LPR (measured from the separate coupon) as a function of time before (ref1, ref2 and ref3) and after the N_2-bubbling was initiated. The text box gives the [HS-] measured with grab samples during the N_2-bubbling.*

3.10 Experiment 10 – 7.5 hrs N_2 bubbling

The stress and elongation as a function of time for Test 4 for H_2 is shown in Figure 3-34, with the [HS^-] concentration. The average strain rate between 1000 and 2000 minutes was about $1.1*10^{-8}$ s^{-1}. An increase in the strain rate is observed almost immediately after the N_2-bubbling was started at a rate of about 0.4-1.0 l/hr. Figure 3-35 shows the same data limited to the time when N_2-bubbling was initiated, showing that the strain rate increased to about $8.6*10^{-7}$ s^{-1} (by about x17), then gradually slowed to about $5.2*10^{-7}$ s^{-1} and finally to about $1.2*10^{-7}$ s^{-1} before the experiment was stopped. The [HS^-] decreased due to the N_2-bubbling from 32 mg/l to 3.5 mg/l during the 7.5 hrs. The corrosion potential of the creep specimen was -0.13 V vs SHE, whereas based on previous measurements at this sulphide concentration the expected value of the corrosion potential would be about -0.6 V vs SHE.

The reason for the much higher than expected corrosion potential of the creep specimen is suggested to be that before this experiment we performed with the same autoclave a tensile test in air at 90°C, which produced an oxide film on the autoclave walls and internals. The oxide film then prevented the autoclave body potential to drop down to the expected level when the autoclave was filled with the sulphide containing water. Simultaneously, the electrical insulation of the creep specimen was rather low, resulting in the creep specimen corrosion potential following closely the autoclave body potential.

What can be learned from this result is that the increase in strain rate does occur (with a slow enough N_2-bubbling rate) in a rather large window of corrosion potentials (keeping in mind that probably the sulphide film in this test had a somewhat different stoichiometry than in a test where the corrosion potential would have been about the expected -0.6 V_{SHE}). This result also suggests that the increase in strain rate is more likely to be caused by injection of vacancies into the Cu-OFP than injection of hydrogen, since it is highly unlikely that hydrogen would be involved in any electrochemical reactions related to the sulphide film reduction supposed to occur as a result of diminishing sulphide concentration in the water at this very high electrochemical potential.

Figure 3-36 shows the LPR measured just before and during the N_2-bubbling period. The current densities were about x10 higher than measured before (see e.g. Figure 3-33 above), reflecting the fact that most of the current arises from the autoclave body and not from the creep specimen. It is also evident that the autoclave body is very slow (at least at this very high potential) in responding to the decrease in the [HS^-] concentration – a clear decrease in the current density is seen only in the two last curves (corresponding to [HS^-] of 6 and 3.5 mg/l). This result further indicates that this experiment can not be considered valid in all respects.

After terminating the test, the specimen was immediately removed from the autoclave and the sulphide film on the gauge length was removed by #220 SiC-paper. The gauge length was cut in two pieces, which were washed by ion pure water, rinsed with ethanol and gently dried by warm air (T < 40°C), after which the two samples were placed in a freezer (at -18°C) awaiting the Hot melt extraction (HME analysis). The time from retrieval of the coupon from the autoclave to transporting it to the freezer was slightly below 20 minutes. The hydrogen concentration measured was 12.9 ppm.

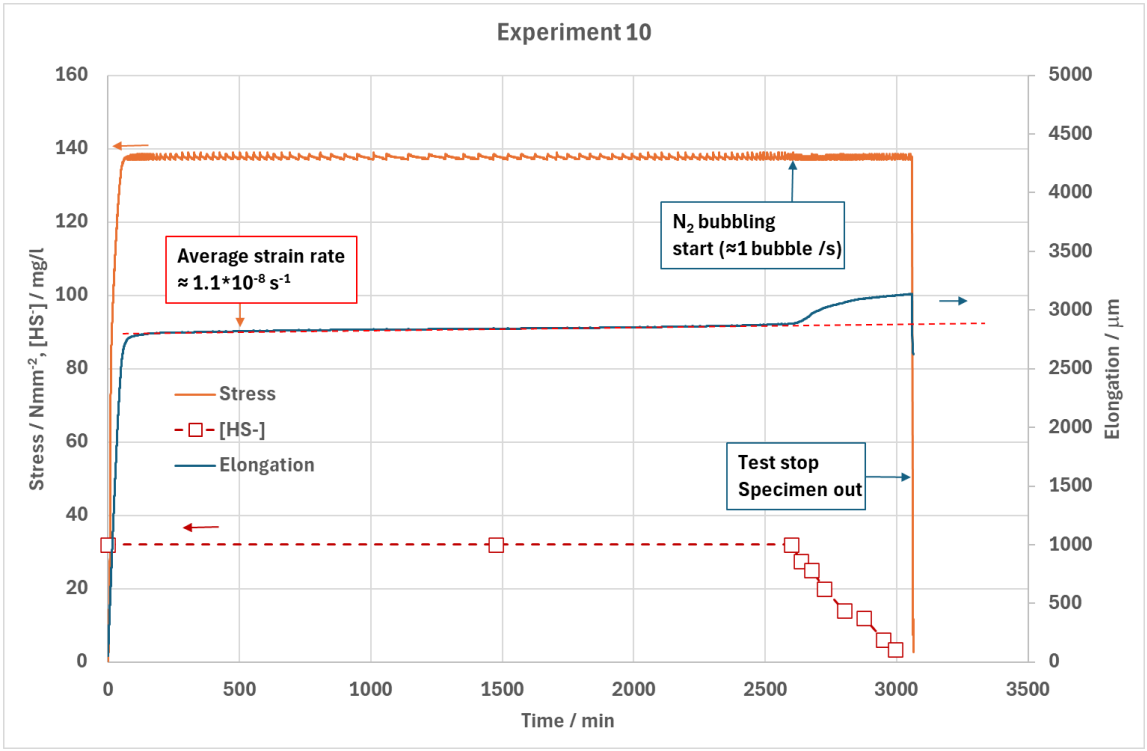

Figure 3-34. *Stress, elongation and [HS⁻] as a function of time, Test 4 for H_2.*

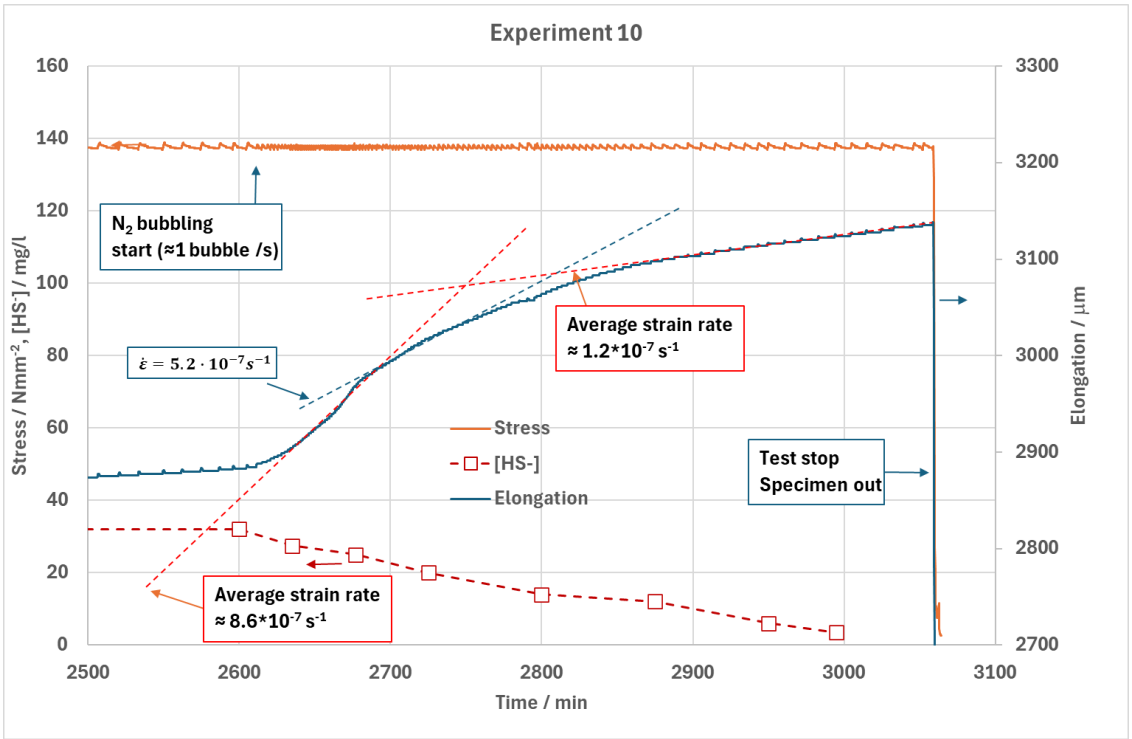

Figure 3-35. *A detail of data shown in Figure 3-34 (time period from 2500 to 3100 min), showing more clearly the effect of starting the N_2-bubbling on the strain rate.*

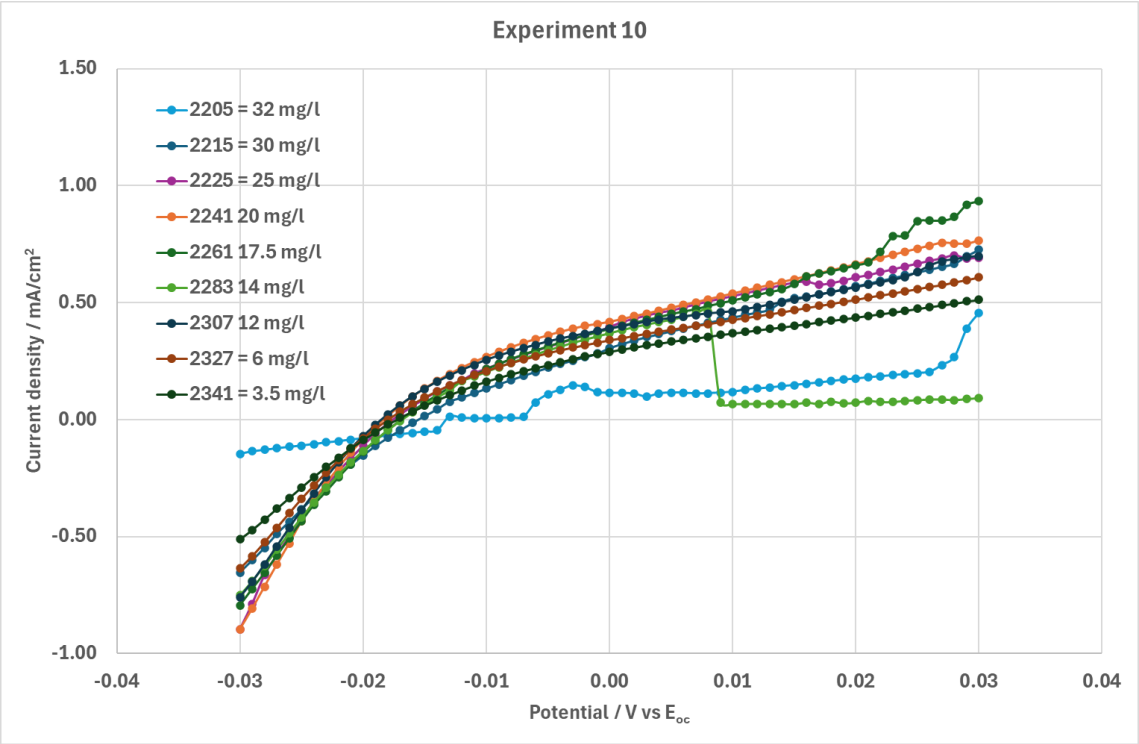

Figure 3-36. *The LPR (measured from the creep specimen) as a function of time before (2205) and after the N_2-bubbling was initiated. The [HS^-] measured with the Vacuettes during the N_2-bubbling are shown after each file number in the labels.*

3.11 Experiment 11 – 6.5 hrs N_2 bubbling

The stress and elongation as a function of time for Test 5 for H_2 is shown in Figure 3-37, with the [HS^-] concentration. An increase in the strain rate is observed almost immediately after the N_2-bubbling was started at a rate of about 0.4 - 1.0 l/hr. Figure 3-38 shows the same data limited to the time when N_2-bubbling was initiated, showing that the strain rate increased from $3.2*10^{-8}$ s^{-1} to about $2.7*10^{-7}$ s^{-1} (by about x8.5), then gradually slowed to about $1.0*10^{-7}$ s^{-1} before the experiment was stopped. The [HS^-] decreased due to the N_2-bubbling from 32 mg/l to 8 mg/l during the 6.5 hrs of N_2-bubbling.

The corrosion potential of the creep specimen, Figure 3-39, was about -0.6 V_{SHE}, at the expected level based on previous measurements at this sulphide concentration. Note that from the time of starting the N_2-bubbling, corrosion potential monitoring was stopped, and the coupon specimen was used to measure the linear polarization resistance (LPR) at frequent intervals. Figure 3-40 shows the LPR measured just before and during the N_2-bubbling period. A trend can be seen where decreasing sulphide concentration is correlated with decreasing current density at the anodic end of the LPR sweep.

After terminating the test, the specimen was immediately removed from the autoclave and the sulphide film on the gauge length was removed by #220 SiC-paper. The gauge length was cut in two pieces, which were washed by ion pure water, rinsed with ethanol and gently dried by warm air (T < 40°C), after which the two samples were placed in a freezer (at -18°C) awaiting the Hot melt extraction (HME analysis). The time from retrieval of the coupon from the autoclave to transporting it to the freezer was slightly below 20 minutes. The hydrogen concentration measured was 16.3 ppm.

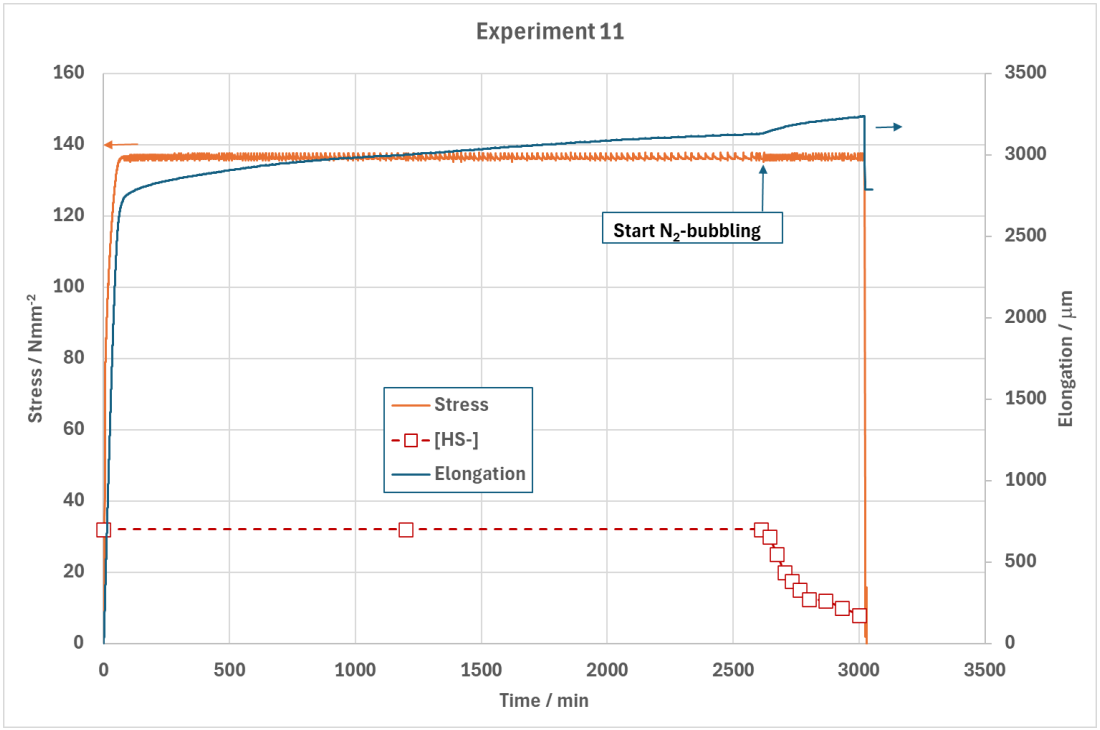

Figure 3-37. *Stress, elongation and [HS⁻] as a function of time, Test 5 for H_2.*

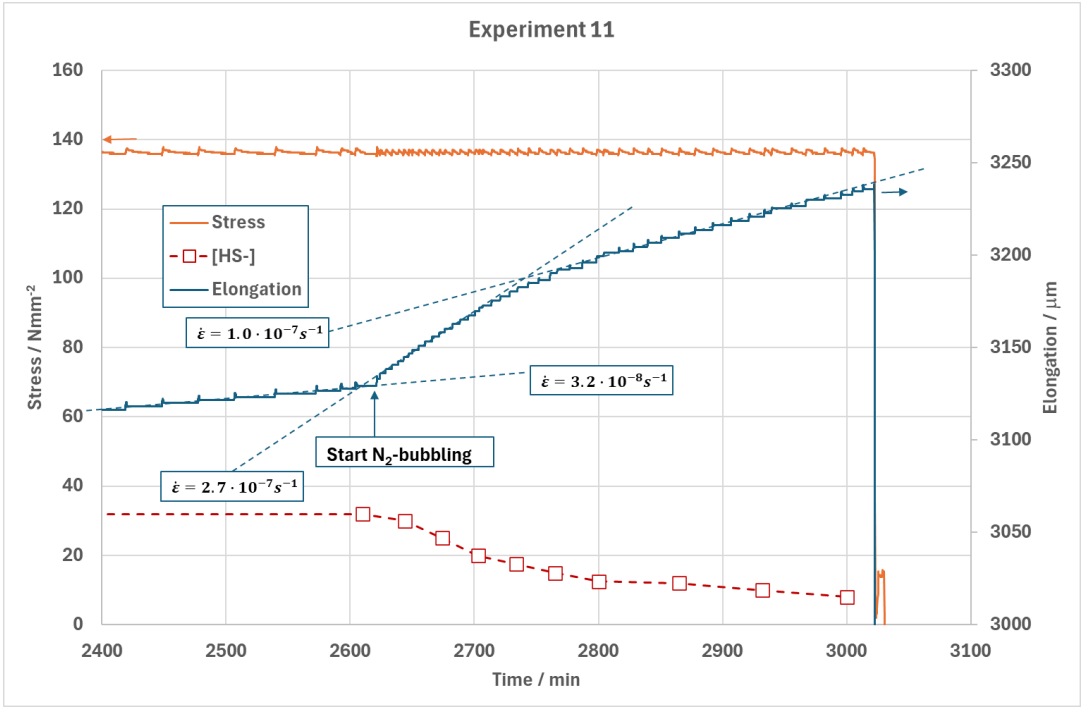

Figure 3-38. *A detail of data shown in Figure 3-37 (time period from 2400 to 3100 min), showing more clearly the effect of starting the N_2-bubbling on the strain rate.*

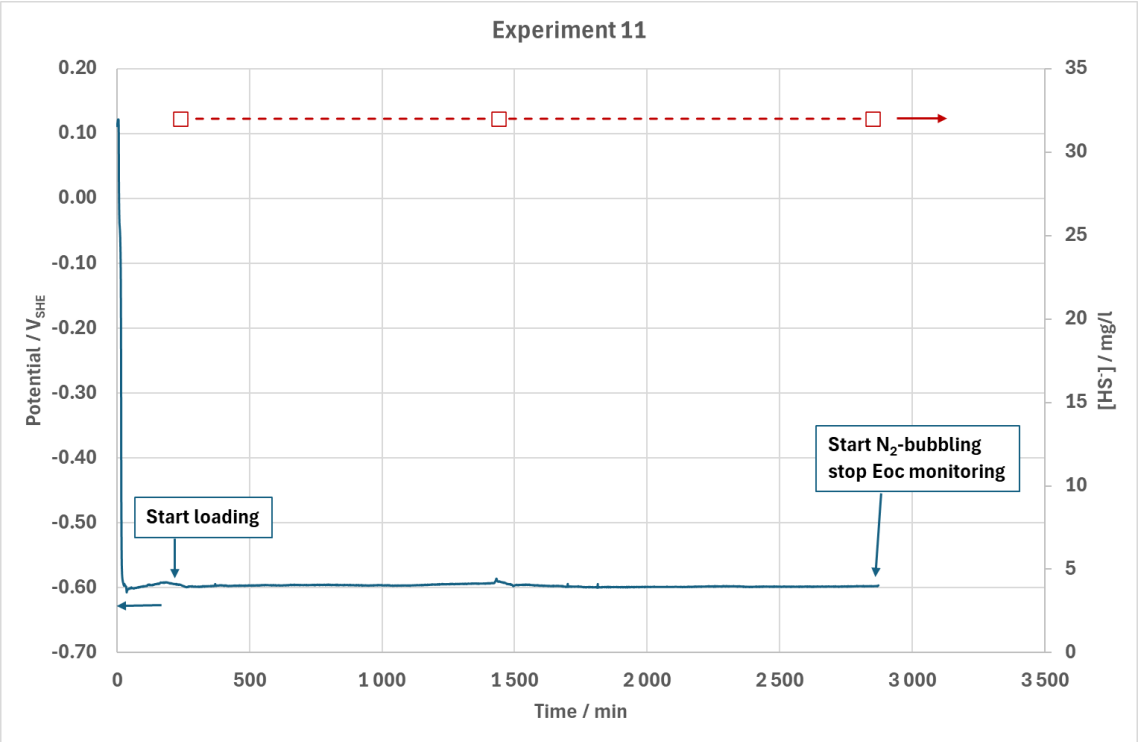

Figure 3-39. *The corrosion potential (V_{SHE}) and [HS^-] (mg/l) as a function of time (until the start of the N_2-bubbling).*

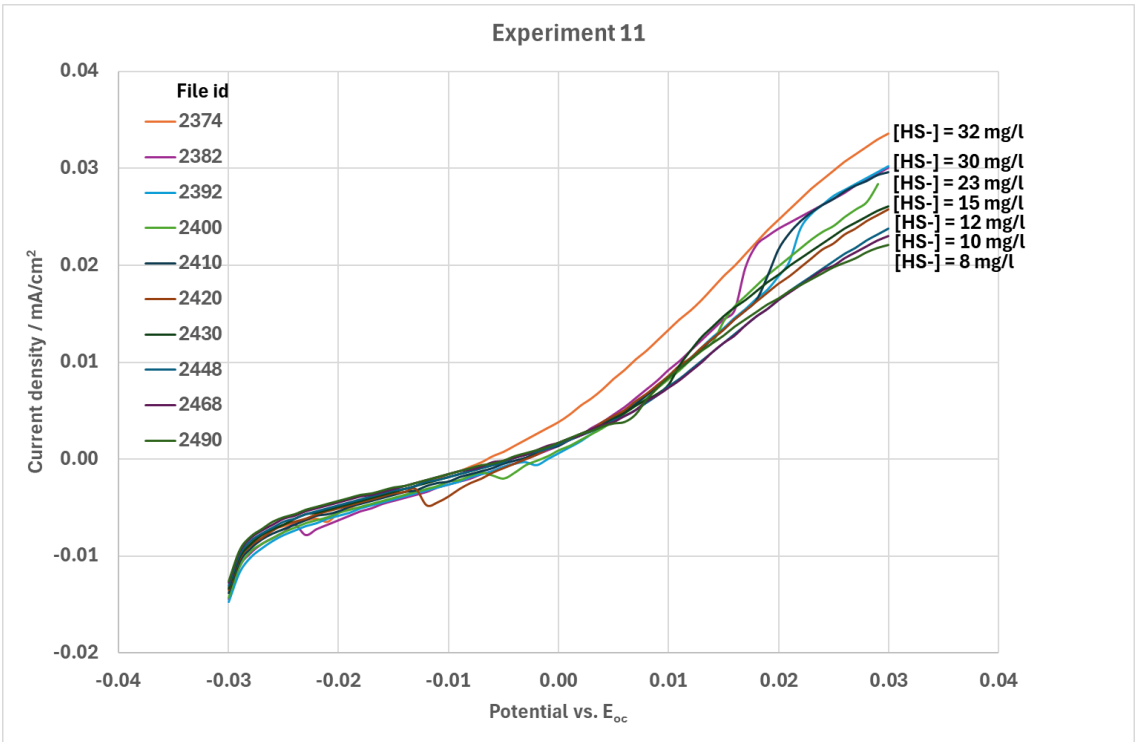

Figure 3-40. *The LPR (measured from the creep specimen) as a function of time before (2374) and after the N_2-bubbling was initiated. The [HS^-] measured with the Vacuettes during the N_2-bubbling are shown at the end of each curve.*

4 Discussion

4.1 Removal rate of sulphide

The results of both Experiments 1 and 2 of the current project, where the sulphide was removed by changing the water into a buffer without sulphide are shown in Figure 4-1, indicating that the increase in the corrosion potential in Experiment 2 was 0.52 mV/min (note that in Experiment 1 the sulphide level did not reach 0 mg/l (but 2 mg/l) due to an error in the experimental procedure, and thus the value of 0.12 mV/min for this test should be taken with a grain of salt). Note that in case of Experiment 2, it took only about 210 min to reduce the sulphide concentration from 30 to 0 mg/l.

The strain rate in Experiment 2 was shown to increase by a factor of only about x2 and return to the base line within about the same time that the sulphide concentration reached 0 mg/l. The strain rate in Experiment 1 also showed an increase in strain rate, by slightly less than x2, and return to the base line timewise similarly as in Experiment 2.

In comparison, from two repetitions of earlier performed tests (report VTT-R-00019-20), where sulphide was removed with N2-bubbling (an example of the test result is shown in Figure 4-2), the change in the corrosion potential as a function of time was close to linear and in the range of 0.01 to 0.07 mV/min. Unfortunately, the sulphide concentration was not measured often enough during these experiments. However, based on the two sulphide measurement points shown in Figure 4-2, it took about 1020 min to reduce the sulphide concentration from 25 to 5.5 mg/l. In addition, it took about 4000 min in both these tests for the strain rate to drop to the base line after the start of removal of sulphide from the water by nitrogen bubbling, i.e. about x20 times longer than when sulphide was removed by replacing water with buffer without sulphide.

Table 4-1 shows the equilibrium potential of Cu/Cu2S as calculated by HSC 6.1 -software for three different sulphide concentrations. The value estimated for [HS-] = 10-3 M is ECu/Cu2S = -0.63 VSHE, suggesting that at the target concentration of HS-, the sample potential resides at the Cu/Cu2S equilibrium potential. In all the test results shown in Figures 4-1 and 4-2, the magnitude of the increase in the corrosion potential as the sulphide concentration decreases can be attributed to the fact that the corrosion potential aligns with the changes in the ECu/Cu2S. Note that this is probably a simplification, since the sulphide film on copper is thought to be at least partially non-stoichiometric.

Table 4-1 The calculated $E_{Cu/Cu2S}$ -potential as a function of the sulphide concentration in the water (HSC 6.1 -software).

[HS-] / M	$E_{Cu/Cu2S}$ / V_{SHE}
10^{-3}	-0.63
10^{-4}	-0.61
10^{-5}	-0.58

Based on the results, removing sulphide from the buffer by N2-bubbling is about x20 times slower than removing it by replacing the water with a buffer without sulphide. This is logical, since in the former process HS- ions in water need to first recombine to gaseous form (H2S) to escape from the autoclave through the outflowing N2 gas stream. In the latter process the recombination reaction is not needed, since HS- is directly carried out from the autoclave in the water phase.

It can therefore be concluded that whatever the process driving the increase in strain rate due to sulphide removal, it has a greater impact on the strain rate when the sulphide is removed from the water more slowly.

Experiment 6 showed that removing an oxide film (formed by anodic polarization to either Cu2O or Cu(OH)2 stability regions) by cathodic polarization did not result in a clear and repeatable effect on the strain rate. This may be explained by hypothesizing that the change in the surface condition brought about by the instantaneous application of the potential is too rapid to allow for the process in question to operate or that the reduction of an oxide film occurs via a different mechanism than that of a sulphide film.

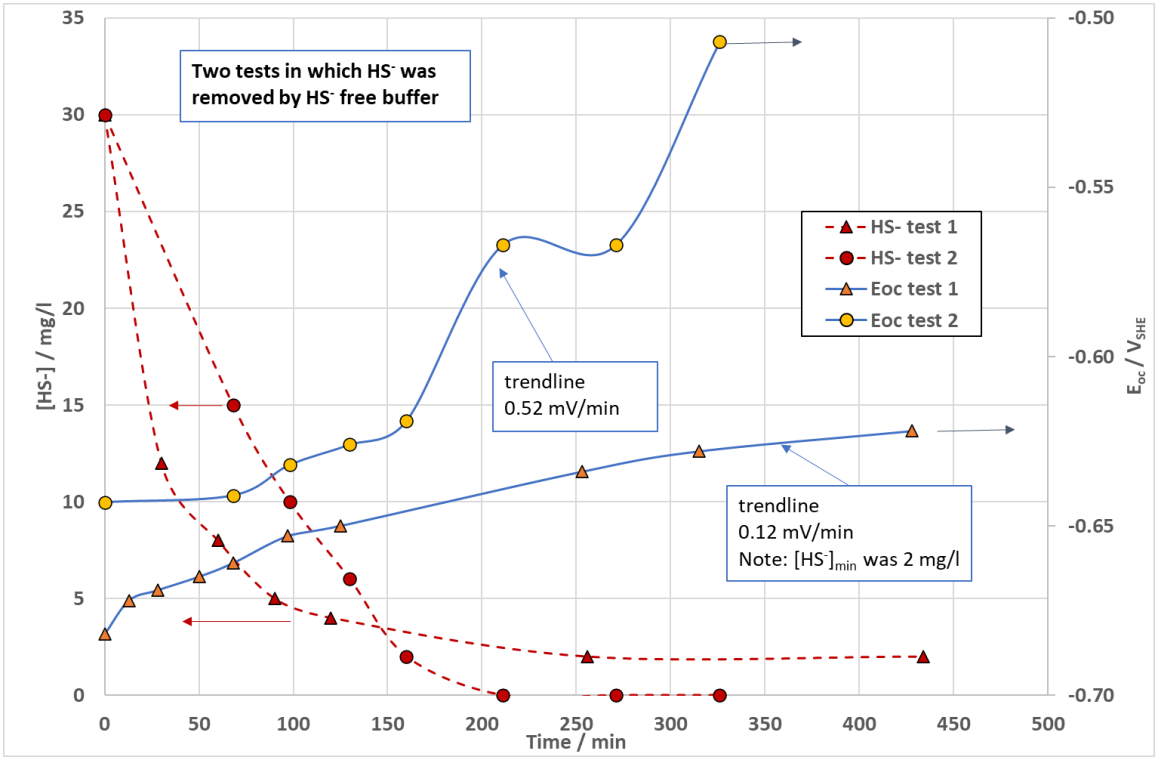

Figure 4-1. *The change in [HS-] and corrosion potential when sulphide was removed by replacing the water with buffer without sulphide (data from Experiments 1 and 2).*

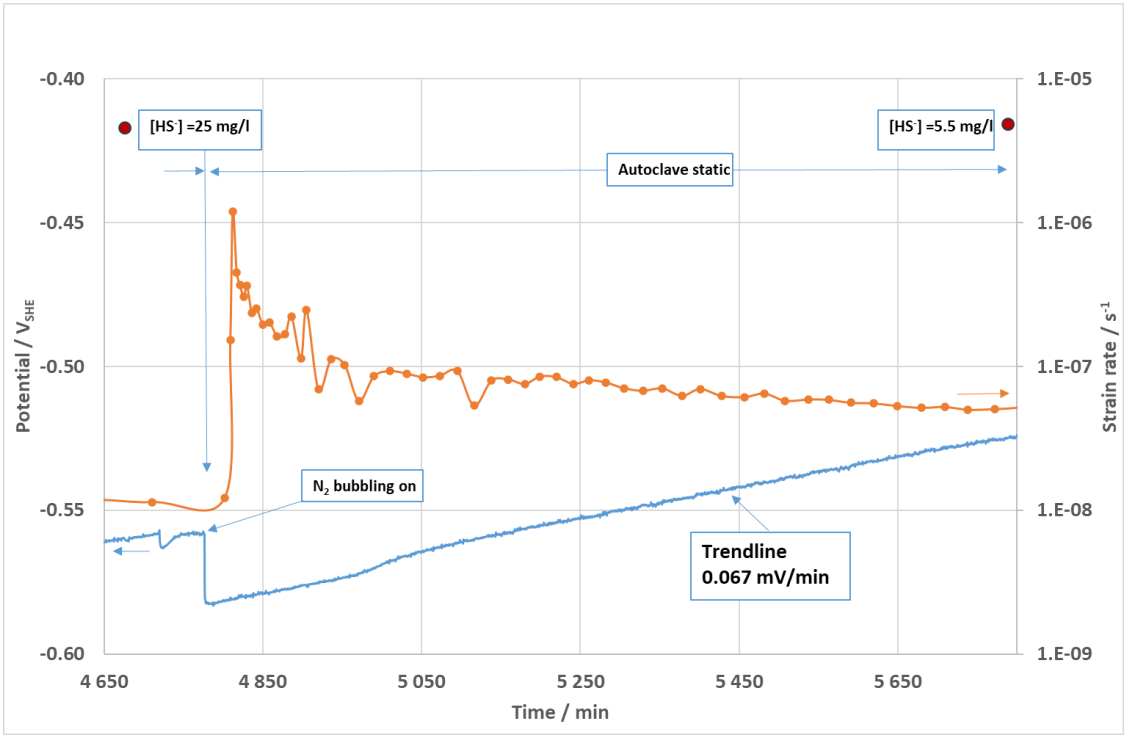

Figure 4-2. *The change in strain rate and corrosion potential when sulphide was removed by N_2-bubbling (data from report VTT-R-00019-20).*

4.2 Hydrogen concentration in specimens

The hydrogen concentrations measured after the interrupted Experiments 7 to 11 as well as the reference samples are shown in Table 4-2. All together five reference samples were measured. The first one (Ref 1) was produced by cutting a small piece of Cu-OFP by hand saw from a larger block. The four following ones (Refs 2 to 5) were produced by the same procedure as the HME samples cut from the gauge length of the creep specimens, i.e. using a fresh creep specimen, removing the EDM affected layer by #220 SiC-paper and cutting the gauge length in two pieces.

It should be noted that in the process of preparing the samples from the gauge length of sulphide exposed creep specimens, in addition to removing the sulphide film also some of the underlaying Cu-OFP material is unavoidably removed. Considering possible hydrogen injection into Cu-OFP during the sulphide film reduction when starting the N2-bubbling process, such injection would be likely to result in a higher concentration of hydrogen in the surface layers of Cu-OFP than in the deeper parts of the creep specimen. Thus, removing the surface layers in the sulphide film removal procedure would inevitably remove also a part of the injected hydrogen.

It is worth noting that the HME equipment was serviced and re-calibrated after measuring samples Ref 1 and samples from Experiments 7 and 8. Figure 4-2 shows the gas calibration curve. After the surprisingly high hydrogen concentrations measured for Ref 2, Ref 3 and samples from Experiments 9 to 11, Table 4-2, an additional calibration check was performed with two separate 0.97±0.05 ppm BAM calibration pieces, resulting in hydrogen concentrations of 0.93 and 1.1 ppm, proving that the equipment was working properly.

As indicated in Table 4-2, two different operators (A and B) were involved with the HME analyses for this project. When interviewed to find possible differences between the sample handling procedures it was revealed that operator A, after taking the samples from the liquid nitrogen container, rinsed the samples with acetone to additionally secure that no debris were attached onto the surface that could affect the HME measurement, while operator B did not use the acetone rinsing. To check if this could cause the differences seen in the hydrogen concentrations, operator A was asked to measure two additional reference samples (Refs 4 and 5) so that with Ref 4 no acetone rinsing was used, while acetone rinsing was used with Ref 5. The hydrogen concentrations measured were rather similar, indicating that the acetone rinsing does not play a role in the results.

Although all specimens were manufactured from the same Cu-OFP block (T58), the specimens from which samples Ref 2 to Ref 5 and Experiments 9 to 11 were extracted were manufactured as a separate order from the manufacturing company, thus probably originating from a different location within the block than samples Ref 1 and Experiments 7 and 8. A rather high variability of the hydrogen concentration in the Cu-OFP tube T58 has been reported earlier (Huotilainen et al. 2022), extending to 6.2 ppm. High variability of the hydrogen concentration in the tested material can thus not be totally excluded at the moment.

In view of the high variability within the HME measurement results, no definite conclusions about the possibility of hydrogen injection into Cu-OFP during the experiments can be made. As shown in Table 4-2, the hydrogen concentration measured for the reference samples varied between 0.95 and 14.2 ppm (average 6.6 ppm), while that measured for the samples from Experiments 7 to 11 varied between 2.5 and 16.3 ppm (average 8.9 ppm).

Table 4-2 The measured hydrogen concentration (by Hydrogen Melt Extraction, HME).

Sample	[H] / ppm	Operator
Ref 1	3.4	A
Ref 2	13.0	B
Ref 3	14.2	B
Ref 4	0.95	A (B)
Ref 5	1.62	A
Exp 7	2.5	A
Exp 8	3.2	A
Exp 9	9.6	B
Exp 10	12.9	B
Exp 11	16.3	B

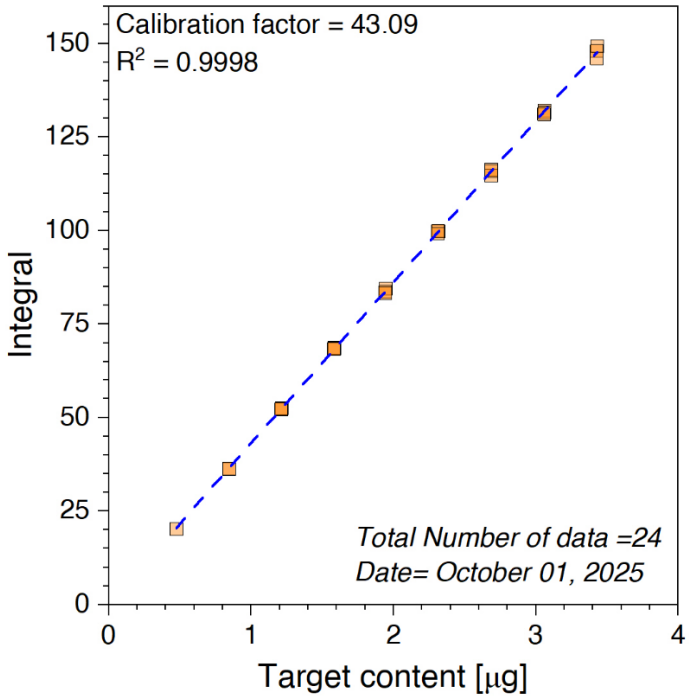

Figure 4-3. *HME gas calibration result.*

Note that in Experiment 10, the corrosion potential of the creep specimen was about -0.13 V_{SHE} instead of the expected (about -0.6 V_{SHE}), due to low insulation resistance allowing the specimen to follow the potential of the body of the autoclave. However, when starting the N_2-bubbling to remove sulphide from the water, an increase in the strain rate by a factor of about x17 was observed. Since at this high potential it would be highly unlikely that hydrogen would be produced in the electrochemical processes related to the sulphide film reduction supposed to occur as a result of diminishing sulphide concentration in the water, the fact that a major creep rate increase was observed strongly indicates that the creep rate increase is caused by vacancies (instead of hydrogen) being injected into Cu-OFP as a result of the sulphide film reduction process.

4.3 LPR data analysis

The anodic branch of linear polarization resistance (LPR) data showed in general a decreasing trend with decreasing sulphide concentration in the water. Figure 4-3 shows the data from four experiments, indicating that there is a relatively high scatter (roughly ±40%) in the current density at each sulphide level. The scatter is suggested, at least to a larger part, arise from the differences in the way sulphide was removed from the buffer in different experiments. For example, in experiment 9, the first LPR measurement at 25 minutes from starting the N2 bubbling showed a current density more than double to that prior to the start of the N2 bubbling, indicating a clear electrochemical activation of the surface. On the other hand, no such activation was observed in Experiments 1 and 2, in which the sulphide was removed by feeding a fresh buffer without sulphide into the autoclave.

A scientific journal paper was published based on these data and the information gained from Experiment 5 (Arstila et al. 2025).

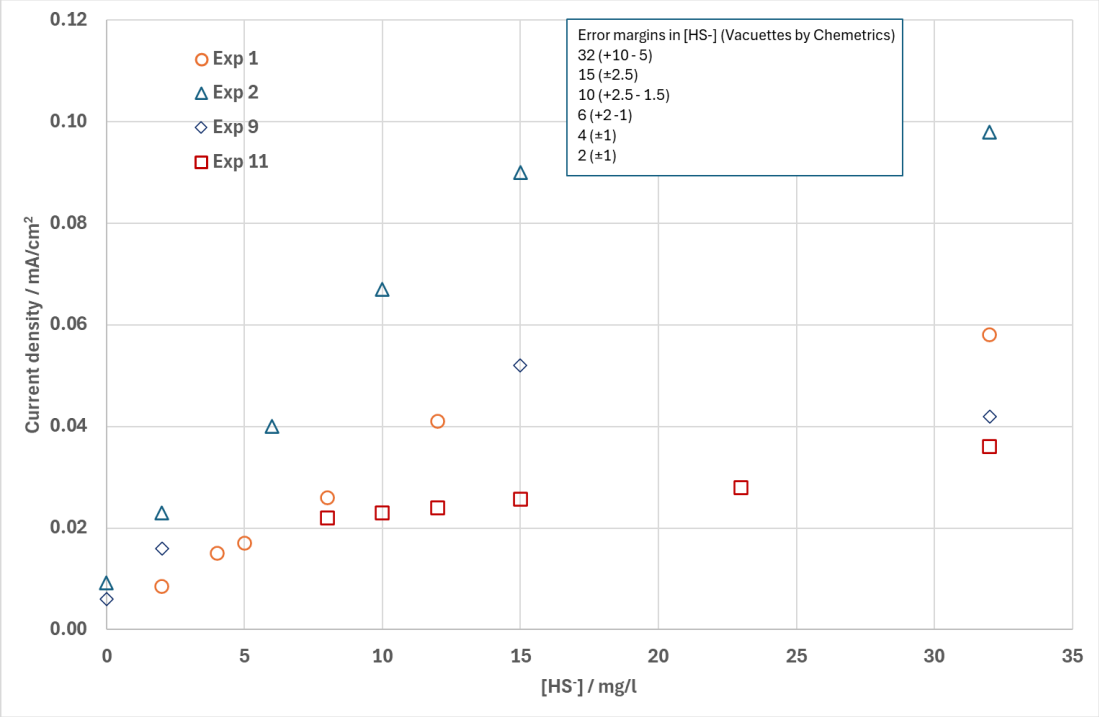

Figure 4-4. *Compilation of LPR data (current density at the highest anodic potential) as a function of [HS$^-$] measured from grab samples. The insert shows the estimated uncertainty in sulphide measurement at six different concentration levels.*

4.4 Source of oxygen rich layer within the sulphide film

In Experiment 5, the target was to find out the source of an oxygen enriched layer within the sulphide film on a Cu-OFP sample previously exposed to sulphide containing water. Such oxygen enriched layer has been repeatably found in samples prepared by conventional metallographic sample preparation techniques involving polishing in water-based solutions.

In this work, when the sample was kept under a nitrogen blanket after exposure to sulphide containing water and the cross-section for SEM investigation was prepared with Focused Ion Beam (FIB) within the SEM vacuum chamber, no evidence for an oxygen enriched layer was found. However, when the cross-section sample was prepared in the normal way in which the sample is in contact with air and water containing dissolved oxygen, an oxygen enriched layer was found.

Thus, it can be concluded that the oxygen enriched layer is an artefact, formed during the normal metallographic sample cross-section preparation procedure. It is hypothesised that the sulphide film being rather porous and not well adhered to the Cu-OFP surface, does not prevent the access of air or water with dissolved oxygen into the sulphide film structure up to the sulphide film – Cu-OFP interface. Also, the atoms at the metal surface are probably at a higher energy and thus more ready to react with oxygen, if available.

4.5 Possible error sources

The experimental set-up is considered to have no influence on the observed increase in creep rate due to removal of sulphide from the water. Based on our experience, any abrupt change in the loading line (failure of grips, loading pins, insulators, or the specimens themselves), would result in an equally abrupt change in the load (since an active load control was used). This has not been observed as seen in the above Figures showing the stress as a function of time.

The fact that the creep rate increase occurs only if N_2 bubbling rate is slow enough indicates that the N_2 bubbling in itself (by mechanical means – e.g. bubbles bouncing on the specimen) does not cause the phenomena. This has been also earlier separately verified by performing a test in pure buffer where initiation of N_2 bubbling did not cause such an increase in creep rate.

5 Conclusions

In this work, the main target was to investigate the source of the creep rate increase in Cu-OFP when exposed to sulphide containing water, occurring when the sulphide is removed from the water. From general grounds it was suggested that there are two possible sources for the phenomena, the first one being hydrogen egress/ingress and the second one injection of vacancies into the Cu-OFP, both capable of influencing the dislocations to produce an increase in the creep rate.

Based on the results from this work, the following conclusions can be made. The main conclusion is that injection of vacancies into Cu-OFP is likely the cause of the observed increase in the creep rate when sulphide removal is started. The kinetics of the process is such that the rate of removal of sulphide from the water becomes an important parameter. Too high a rate of sulphide removal, such as having too high a bubbling rate of N_2 or replacing the sulphide containing water with fresh water without sulphide, shows only a small or negligible increase in the creep rate. The N_2 bubbling by itself (i.e. through a mechanical action on the specimen) was shown not to produce a significant effect on the creep rate.

The oxygen enriched layer at the sulphide film – Cu-OFP interface observed by several research groups was shown to be caused by an artefact. The sulphide film is of a porous nature, allowing ingress of oxygen into the sulphide film – Cu-OFP interface during the post-exposure SEM sample preparation process.

As a separate finding of this work, the anodic current density of Cu-OFP at a potential 30 mV positive to the corrosion potential was found to correlate well with the sulphide concentration in the water (up to about 20 mg/l), thus providing a possible on-line sensor for sulphide concentration monitoring during experiments.

6 References

SKB's (Svensk Kärnbränslehantering AB) publications can be found at www.skb.com/publications. SKBdoc documents will be submitted upon request to document@skb.se.

Arstila K, Bergendal E, Chonche A, Ikäläinen T, Lilja, C, Que Z, Saario T, 2025. Oxide formation at the sulfide film-copper interface in anoxic sulfide solution and on-line sulfide detection via linear polarization resistance. First published: 15 October 2025. https://doi.org/10.1002/maco.70067

Huotilainen C, Hytönen N, Saario T, 2022. Hydrogen in Cu-OFP, VTT Research Report VTT-R-00048-22, SKBdoc 1977155, version 1.0.

Ikäläinen T, Saario T, Que Z, 2022. Creep rate in Cu-OFP under applied electrochemical potential and presence of sulphide, SKB TR-22-05, Swedish Nuclear Fuel and Waste Management Co (SKB).

Lilja C, 2021. Calculated by the Spana software of KTH.

Välimäki T, 2009. SKB T58 tube structure evaluation. Luvata Pori Oy Report 1.6.2009. SKBdoc 1216615, version 2.0.